Dnmt2 mediates intergenerational transmission of paternally acquired metabolic disorders through sperm small non-coding RNAs

Yunfang Zhang [1,2,3,8], Xudong Zhang [2,8], Junchao Shi [2,8], Francesca Tuorto [4,8], Xin Li[1,8], Yusheng Liu[1], Reinhard Liebers[4], Liwen Zhang[1,3], Yongcun Qu[1,3], Jingjing Qian[1,3], Maya Pahima[2], Ying Liu[2], Menghong Yan[5], Zhonghong Cao[1,6], Xiaohua Lei[1], Yujing Cao[1], Hongying Peng[2], Shichao Liu[2], Yue Wang[2], Huili Zheng[2], Rebekah Woolsey[7], David Quilici[7], Qiwei Zhai[5], Lei Li [1], Tong Zhou[2], Wei Yan[2], Frank Lyko [4], Ying Zhang [1*], Qi Zhou [1*], Enkui Duan [1*] and Qi Chen [2*]

The discovery of RNAs (for example, messenger RNAs, non-coding RNAs) in sperm has opened the possibility that sperm may function by delivering additional paternal information aside from solely providing the DNA[1]. Increasing evidence now suggests that sperm small non-coding RNAs (sncRNAs) can mediate intergenerational transmission of paternally acquired phenotypes, including mental stress[2,3] and metabolic disorders[4–6]. How sperm sncRNAs encode paternal information remains unclear, but the mechanism may involve RNA modifications. Here we show that deletion of a mouse tRNA methyltransferase, DNMT2, abolished sperm sncRNA-mediated transmission of high-fat-diet-induced metabolic disorders to offspring. *Dnmt2* deletion prevented the elevation of RNA modifications (m^{5}C, m^{2}G) in sperm 30–40 nt RNA fractions that are induced by a high-fat diet. Also, *Dnmt2* deletion altered the sperm small RNA expression profile, including levels of tRNA-derived small RNAs and rRNA-derived small RNAs, which might be essential in composing a sperm RNA 'coding signature' that is needed for paternal epigenetic memory. Finally, we show that Dnmt2-mediated m^{5}C contributes to the secondary structure and biological properties of sncRNAs, implicating sperm RNA modifications as an additional layer of paternal hereditary information.

It is now widely accepted that hereditary information in the germline can be encoded in forms other than merely the DNA sequence[1,7]. For example, in mammalian sperm, non-DNA sequence-based hereditary information carriers could be chemical marks associated with DNA (that is, DNA methylation and histone modifications[8–10]) as well as diffusible molecules such as small non-coding RNAs (sncRNAs)[1,11]. All have the potential to encode and store paternally acquired information, possibly in a synergistic manner[1,7,11]. Of particular interest, sncRNAs are mobile and can act in trans, making them good candidates for encoding paternal information and for interacting with other information carriers[1,11].

Recently, zygotic injection of isolated sperm total RNAs or a subset of sperm sncRNAs has provided direct causal evidence for a role of sperm RNAs in intergenerational transmission of paternally acquired phenotypes, including mental stress[2,3] and metabolic disorders[4,5].

We have previously demonstrated that the 30–40 nt sperm RNA fraction, predominantly consisting of tRNA-derived small RNAs (tsRNAs; also known as tRNA-derived fragments, tRFs), contains essential paternal information, and that injection of this 30–40 nt sperm RNA fraction could confer high-fat-diet (HFD)-induced paternal metabolic disorders to the offspring[4]. In addition, we found multiple types of RNA modification in sperm RNAs that contribute to RNA stability[4], and that certain RNA modifications (m^{5}C and m^{2}G) were elevated in the 30–40 nt sperm RNA fractions under paternal HFD conditions[4]. Also, zygotic injection of unmodified tRNA/tsRNAs failed to induce offspring phenotypes that can be exerted by modified RNAs purified from tissues[4,12]. These data, together with other reports[13], suggest that RNA modifications may represent an additional layer of information that contributes to sperm RNAs' identity as an 'epigenetic information carrier'[1,14]. Here we report that DNMT2-mediated RNA modification and sperm sncRNA expression profiles are required for the establishment of a sperm RNA 'coding signature' and for intergenerational transmission of paternally acquired metabolic disorders induced by a HFD.

DNMT2 is a multisubstrate tRNA methyltransferase[15] that has been reported to methylate the C38 position (m^{5}C) of tRNA-Asp, tRNA-Gly and tRNA-Val[16,17]. The loss of m^{5}C at C38 can facilitate tRNA fragmentation, which leads to excessive amounts of tsRNAs and may elicit pathophysiological conditions[17,18]. Indeed, we observed that *Dnmt2*$^{-/-}$ sperm showed upregulated levels of tsRNA-Gly (Supplementary Fig. 1a), which is one of the most abundant types of tsRNA in sperm[4,6,19]. Moreover, we found that a HFD can induce upregulated *Dnmt2* expression in the caput epididymis (Supplementary Fig. 1b), a segment of male reproductive tract
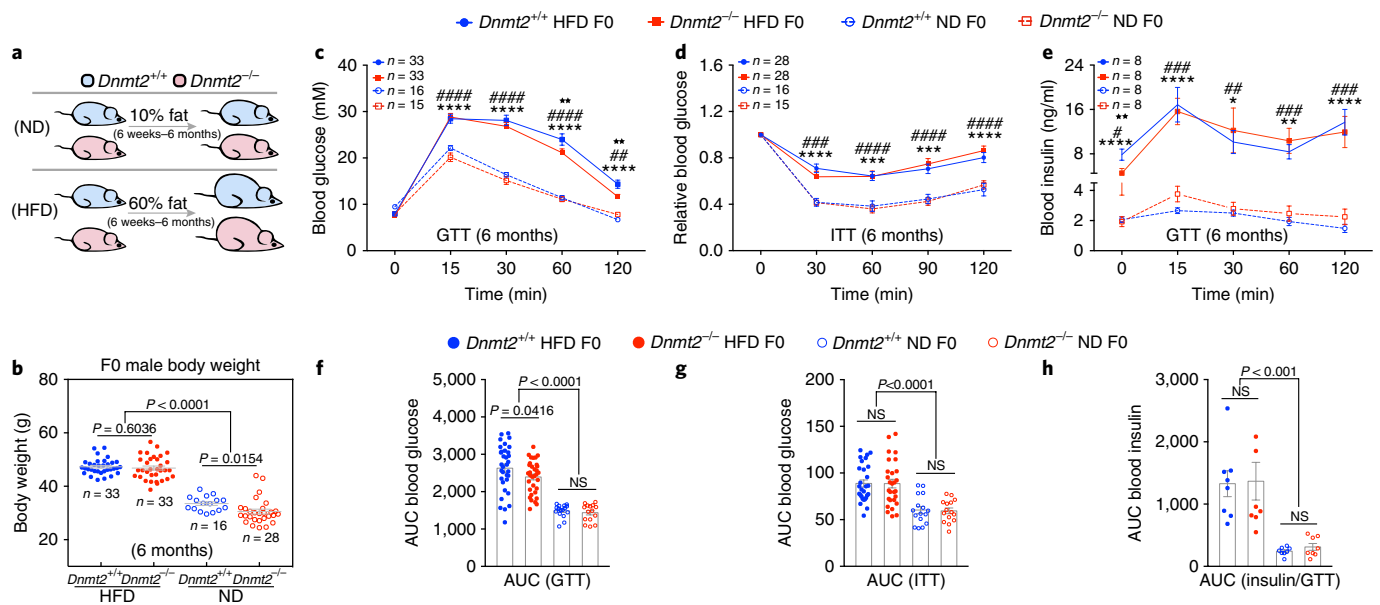
535

Fig. 1 | Body weight and metabolic parameters of F0 males (*Dnmt2*+/+ and *Dnmt2*−/−) under HFD and ND. *n* = number of mice in each group. **a**, *Dnmt2*+/+ and *Dnmt2*−/− F0 males were fed a ND (10% fat) or HFD (60% fat) from the age of 6 weeks to 6 months. **b**, Body weight of F0 males in each group at 6 months of age. Each dot represents one mouse, data pooled from seven experiments. Statistical analysis was performed by two-tailed, one-way analysis of variance (ANOVA), uncorrected Fisher's least significant difference (LSD). **c**, Blood glucose during the GTT. Data are pooled from seven experiments. Statistical analysis was performed by two-tailed, two-way ANOVA, uncorrected Fisher's LSD. ****$P < 0.0001$ (*Dnmt2*+/+ HFD versus *Dnmt2*+/+ ND); ##$P < 0.01$, ####$P < 0.0001$ (*Dnmt2*−/− HFD versus *Dnmt2*−/− ND); **$P < 0.01$ (*Dnmt2*+/+ HFD versus *Dnmt2*−/− HFD). **d**, Relative blood glucose during the ITT. Data are pooled from seven experiments. Statistical analysis was performed by two-tailed, two-way ANOVA, uncorrected Fisher's LSD. ***$P < 0.001$, ****$P < 0.0001$ (*Dnmt2*+/+ HFD versus *Dnmt2*+/+ ND); ###$P < 0.001$, ####$P < 0.0001$ (*Dnmt2*−/− HFD versus *Dnmt2*−/− ND). **e**, Serum insulin during the GTT. Data are pooled from four experiments. Statistical analysis was performed by two-tailed, two-way ANOVA, uncorrected Fisher's LSD. *$P < 0.05$, **$P < 0.01$ ****$P < 0.0001$ (*Dnmt2*+/+ HFD versus *Dnmt2*+/+ ND); #$P < 0.05$, ##$P < 0.01$, ###$P < 0.001$, **$P < 0.01$ (*Dnmt2*−/− HFD versus *Dnmt2*−/− ND). **f–h**, Area under the curve (AUC) statistics for **c**, **d** and **e**, respectively. Statistical analysis was performed by two-tailed, one-way ANOVA, uncorrected Fisher's LSD. NS, not significant. All data are plotted as mean ± s.e.m. All statistical source data and *P* values are provided in Supplementary Table 1.

where sperm undergo maturation and there is fine-tuning of sperm tsRNA composition[6]. *Dnmt2* upregulation in the caput epididymis also coincides with an increased level of m5C in sperm 30–40 nt RNA fractions, as we previously reported[4]. These converging clues suggest that DNMT2-mediated RNA modifications and tsRNA biogenesis may represent a previously unidentified mechanism to encode paternal information (for example, those induced by a HFD) in sperm RNAs.

To study the potential involvement of DNMT2 in the process of intergenerational transmission of HFD-induced metabolic phenotypes, we first backcrossed the *Dnmt2* strain (imported from Jax® mice) into C57BL/6NCrl background (Supplementary Fig. 1c), then fed *Dnmt2*−/− and *Dnmt2*+/+ males a HFD (60% fat) or a normal diet (ND, 10% fat) from 6 weeks to 6 months of age (Fig. 1a). We examined their weight and metabolic parameters at age 6 months (Fig. 1b–h). Under ND condition, the *Dnmt2*−/− males showed a slightly, but statistically significant lower body weight than *Dnmt2*+/+ males (Fig. 1b), with similar metabolic parameters, as revealed by a glucose tolerance test (GTT) and insulin tolerance test (ITT) (Fig. 1c–h and Supplementary Table 1). Under HFD condition, body weight was comparable between *Dnmt2*−/− and *Dnmt2*+/+ males, with both groups becoming obese (Fig. 1b), glucose intolerant and insulin resistant, in contrast to the ND groups (Fig. 1c–h and Supplementary Table 1). The glucose intolerance phenotype was comparably milder in *Dnmt2*−/− HFD than in *Dnmt2*+/+ HFD males (Fig. 1c and Supplementary Table 1), possibly related to altered adipogenesis in *Dnmt2*−/− mice[18].

To assess whether the sperm RNAs of *Dnmt2*−/− HFD-fed males can pass the paternal metabolic phenotype to their offspring, we used the *Dnmt2*+/+ ND, *Dnmt2*+/+ HFD, *Dnmt2*−/− ND and *Dnmt2*−/−

HFD models, as generated above, and a previously established zygotic sperm RNA injection protocol[4]. We purified total RNAs from the sperm of *Dnmt2*+/+ ND, *Dnmt2*+/+ HFD, *Dnmt2*−/− ND and *Dnmt2*−/− HFD males and injected them into normal zygotes, with the injection of water as a control (because the RNAs injected in the other four groups were dissolved in water) (Supplementary Fig. 1d). RNA injection does not adversely affect embryo development compared with control injection (Supplementary Table 2). The obtained F1 male offspring from the above five groups were fed a ND diet and were examined for body weight and metabolic parameters, beginning at 16 weeks of age (Fig. 2a–d,i–k). The body weights of F1 male offspring in all groups were comparable overall, with a slight, but significant, increase observed in those derived from the *Dnmt2*+/+ HFD group (Fig. 2a and Supplementary Table 1). GTT and ITT analyses revealed that the F1 male offspring generated by the injection of sperm total RNAs from *Dnmt2*+/+ HFD males showed glucose intolerance, but not insulin resistance, when compared with the *Dnmt2*+/+ ND, *Dnmt2*−/− ND and control injection groups (Fig. 2b–d,i–k and Supplementary Table 1). However, male offspring generated by the injection of sperm total RNAs from *Dnmt2*−/− HFD males did not exhibit any obvious metabolic disorders as determined by GTT and ITT, similar to *Dnmt2*+/+ ND, *Dnmt2*−/− ND and control injection groups (Fig. 2b–d,i–k and Supplementary Table 1).

Because we previously demonstrated that the 30–40 nt sperm RNA fraction (predominantly tsRNAs) is the functional component that can efficiently confer paternal phenotypes[4], we next collected the 30–40 nt sperm RNA fractions from *Dnmt2*+/+ ND, *Dnmt2*+/+ HFD, *Dnmt2*−/− ND and *Dnmt2*−/− HFD males, performed zygotic injections (Supplementary Fig. 1e), and examined the body weight and metabolic parameters of the male F1 offspring, beginning at
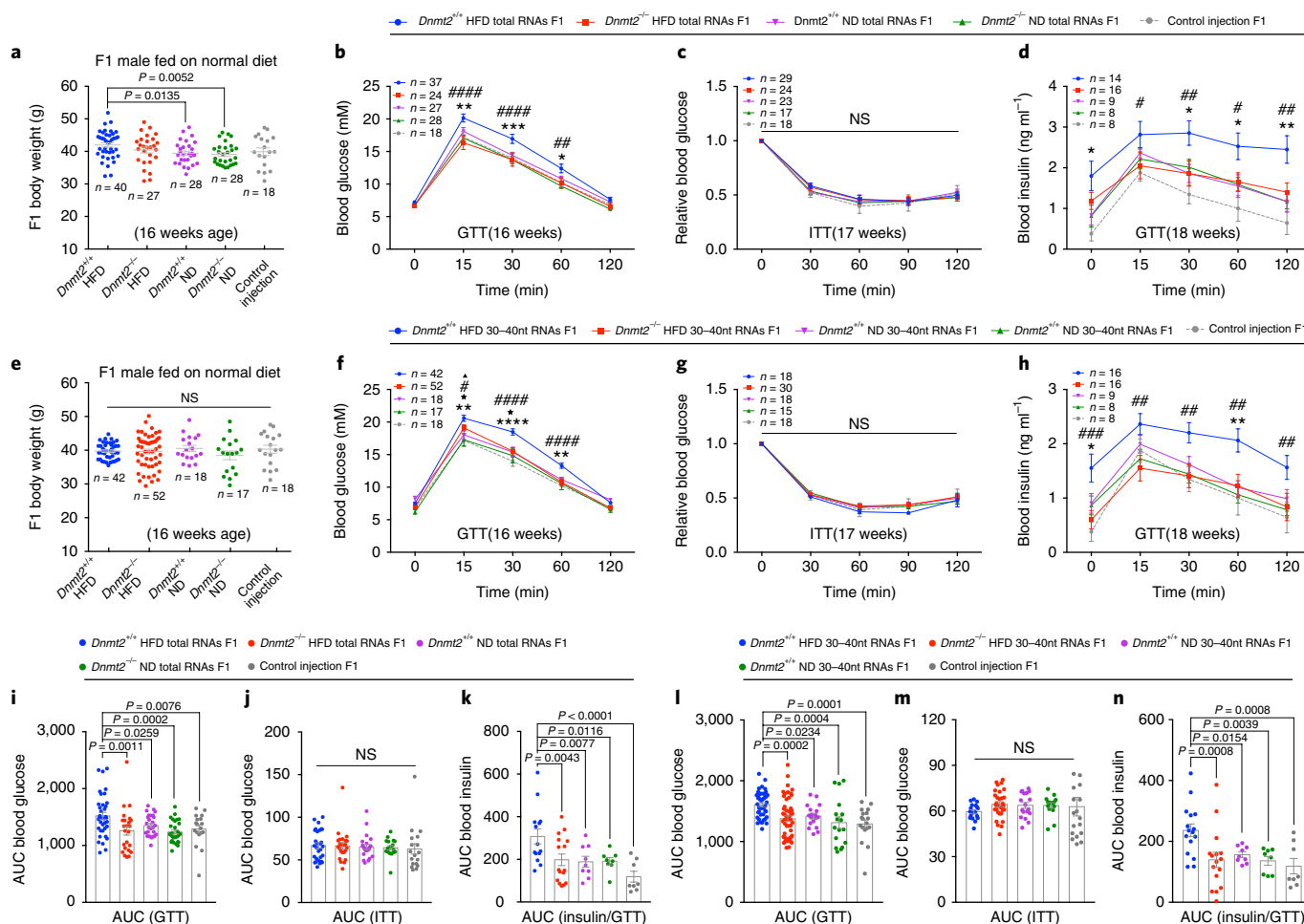
Fig. 2 | Body weight and metabolic parameters of F1 males generated by zygotic injection of sperm total RNAs or 30–40 nt RNAs, fed on a ND. a–d, Body weight and metabolic phenotypes of F1 males generated from injection of sperm total RNAs: body weight (**a**); blood glucose during GTT (**b**); relative blood glucose during ITT (**c**); serum insulin during GTT (**d**). n = number of mice in each group. In **a**, each dot represents one mouse; data are pooled from 10 experiments. In **b**, data are pooled from 10 experiments; *$P < 0.05$, **$P < 0.01$, ***$P < 0.001$ ($Dnmt2^{+/+}$ HFD F1 versus $Dnmt2^{+/+}$ ND F1); ##$P < 0.01$, ####$P < 0.0001$ ($Dnmt2^{+/+}$ HFD F1 versus $Dnmt2^{-/-}$ HFD F1). In **c**, data are pooled from eight experiments. NS, not significant. In **d**, data are pooled from seven experiments; *$P < 0.05$, **$P < 0.01$ ($Dnmt2^{+/+}$ HFD F1 versus $Dnmt2^{+/+}$ ND F1); #$P < 0.05$, ##$P < 0.01$ ($Dnmt2^{+/+}$ HFD F1 versus $Dnmt2^{-/-}$ HFD F1). **i–k**, AUC statistics for **b,c,d**, respectively. NS, not significant. **e–h**, Body weight and metabolic phenotypes of F1 males generated from sperm 30–40 nt RNAs injection: body weight (**e**); blood glucose during GTT (**f**); relative blood glucose during ITT (**g**); serum insulin during GTT (**h**). In **e**, each dot represents one mouse, and data are pooled from 10 experiments; NS, not significant. In **f**, data are pooled from 10 experiments; **$P < 0.01$, ****$P < 0.0001$ ($Dnmt2^{+/+}$ HFD F1 versus $Dnmt2^{+/+}$ ND F1); #$P < 0.05$, ####$P < 0.0001$ ($Dnmt2^{+/+}$ HFD F1 versus $Dnmt2^{-/-}$ HFD F1); ▲$P < 0.05$ ($Dnmt2^{-/-}$ HFD F1 versus $Dnmt2^{-/-}$ ND F1); ★$P < 0.05$ ($Dnmt2^{-/-}$ HFD F1 versus control injection F1). In **g**, data are pooled from seven experiments; NS, not significant. In **h**, data are pooled from seven experiments; *$P < 0.05$, **$P < 0.01$ ($Dnmt2^{+/+}$ HFD F1 versus $Dnmt2^{+/+}$ ND F1); ##$P < 0.01$, ###$P < 0.001$ ($Dnmt2^{+/+}$ HFD F1 versus $Dnmt2^{-/-}$ HFD F1). **l,m,n**, AUC statistics for **f,g,h**, respectively; NS, not significant. All data are plotted as mean ± s.e.m. Statistical analyses were performed by two-tailed, one-way ANOVA (**a,e,i–n**) or two-way ANOVA (**b–d,f–h**), uncorrected Fisher's LSD. NS, not significant. All statistic source data and P values are provided in Supplementary Table 1.

16 weeks of age (Fig. 2e–h,l–n). We found similar body weights in all F1 groups that were fed on a ND (Fig. 2e and Supplementary Table 1). The F1 male offspring of the $Dnmt2^{+/+}$ HFD group showed impaired glucose metabolism, as represented by the significantly higher glucose and insulin levels during GTT compared with $Dnmt2^{+/+}$ ND, $Dnmt2^{-/-}$ ND and control injection groups (Fig. 2f–h,l–n and Supplementary Table 1). In contrast, the F1 male offspring from the $Dnmt2^{-/-}$ HFD group did not show metabolic disorders when compared with the $Dnmt2^{+/+}$ HFD group, but a similar pattern to that of $Dnmt2^{+/+}$ ND, $Dnmt2^{-/-}$ ND and control injection groups (Fig. 2f–h,l–n, Supplementary Fig. 1f,g and Supplementary Table 1), with only a relatively mild increase in glucose levels during GTT at 15 and 30 min time points (Fig. 2f and Supplementary Table 1). Together, data from zygotic injection of both sperm total

RNAs and 30–40 nt RNA fractions (Fig. 2) strongly suggest that $Dnmt2$ deletion in HFD males abolished the ability of sperm RNAs to induce offspring metabolic phenotypes. On the other hand, it is important to note that natural mating of $Dnmt2^{-/-}$ HFD males with $Dnmt2^{-/-}$ ND females can result in transfer of metabolic disorders to their F1 male offspring (Supplementary Fig. 1h–m and Supplementary Table 1), which reinforced the notion that paternally acquired information in sperm can also be encoded by mechanisms other than RNAs[4], and in a $Dnmt2$-independent manner. Other mechanisms that may transfer paternal information to the offspring include histone modifications, rDNA copy variations and DNA methylation in mammals[10,20–22] and other model systems[23–27].

The observed effects of sperm RNAs from $Dnmt2^{-/-}$ HFD could be due to altered RNA modifications, so we next systematically ana-
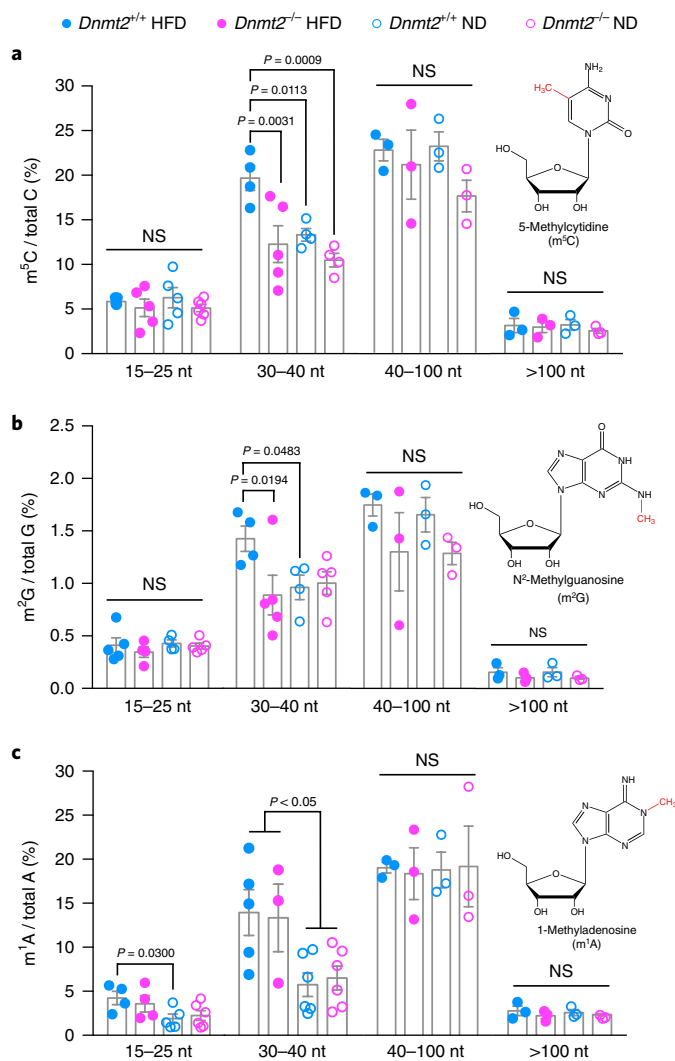
Fig. 3 | Altered RNA modifications in different sperm RNA fractions from F0 *Dnmt2*+/+ and *Dnmt2*-/- males under ND and HFD. a, Relative level of m5C in different sperm RNA fractions (15–25, 30–40, 40–100 and > 100 nt). **b**, Relative level of m2G in different sperm RNA fractions (15–25 nt, 30–40 nt, 40–100 nt and >100 nt). **c**, Relative level of m1A in different sperm RNA fractions (15–25, 30–40, 40–100 and >100 nt). Values for each dot are generated from pooled sperm RNAs from eight mice, to reach the optimal RNA amount in each fraction to perform LC-MS/MS. All data are plotted as mean ± s.e.m., and *n* = number of biologically independent experiments (each dot in the figure represents one experiment), as detailed in Supplementary Table 1. All statistical analysis was performed by two-tailed, one-way ANOVA, uncorrected Fisher's LSD. NS, not significant. All statistic source data and *P* values are provided in Supplementary Table 1.

lysed the RNA modification levels of different fractions of sperm RNAs (15–25, 30–40, 40–100 and >100 nt fractions) from *Dnmt2*-/- HFD, *Dnmt2*+/+ HFD, *Dnmt2*-/- ND and *Dnmt2*+/+ ND males using our previously developed lipid chromatography–tandem mass spectroscopy (LC-MS/MS) protocol[4], which was further modified to improve detection efficiency[28] (see Methods). With this comprehensive approach, we effectively quantified 13 types of sperm RNA modification, and found that a majority of the RNA modifications remained unchanged in the >100 nt RNA fraction between all four groups (Fig. 3, Supplementary Fig. 2 and Supplementary Table 1). This is consistent with previous reports that DNMT2 does not affect RNA modifications in large RNAs[16]. The most significant changes in RNA modifications were observed in the 30–40 nt fractions, where

levels of m5C, m2G and m1A were increased under HFD conditions (Fig. 3 and Supplementary Table 1). The levels of m5C and m2G, but not m1A, were restored to levels comparable to ND mice upon *Dnmt2* deletion (Fig. 3 and Supplementary Table 1). Increased levels of m1A may be associated with the elevated glucose levels under HFD conditions but are probably regulated by enzymes other than DNMT2[29]. The restored level of m5C and m2G in the 30–40 nt sperm RNA fractions under HFD conditions by *Dnmt2* deletion is interesting, and can be explained by two potential mechanisms: (1) the lack of DNMT2 activity in *Dnmt2*-/- males could result in the hypomethylation of tRNAs, as bisulfite sequencing of the three known tRNA targets of DNMT2 in the testis[17] (Supplementary Fig. 4a) and sperm (Fig. 4a) showed a specific loss of m5C at C38; (2) *Dnmt2* deletion could cause a global change in sperm small RNA profiles in the 30–40 nt fraction, with the observed changes in RNA modifications reflecting a secondary effect caused by altered expression profiles of tsRNA or other small RNA subpopulations that harbour related RNA modifications. This second possibility is supported by the fact that there is no evidence to support a direct methylation effect of DNMT2 on m2G, and that *Dnmt2* deletion can increase the fragmentation of tRNAs into tsRNAs[18], as we observed that sperm tsRNA-Gly is elevated upon Dnmt2 deletion under both ND and HFD conditions (Fig. 4b and Supplementary Fig. 1a). Interestingly, we also found that in addition to increasing the tsRNA level in sperm, deletion of *Dnmt2* seems to decrease the level of a recently discovered rRNA-derived small RNA[30] (rsRNA-28S), which is also found in our sperm RNA-seq data (Supplementary Fig. 3), as shown by northern blot (Fig. 4b). Because our recent report showed that *Dnmt2* deletion does not cause hypomethylation of m5C in rRNAs[31], the observed effect of DNMT2 on rsRNAs suggests unknown mechanisms independent of m5C, which is an interesting direction that deserves future investigation.

Finally, we also explored the potential impact of Dnmt2-mediated m5C38 on RNA secondary structures and function. To this end, three types of chemically synthesized tsRNAs were used (Fig. 4c and Supplementary Fig. 4b): (1) 3′tsRNA-Gly harbouring five m5C, representing the *Dnmt2*+/+ condition; (2) 3′tsRNA-Gly with four m5C, lacking the Dnmt2-dependent m5C at C38 and thus representing the *Dnmt2*-/- condition; and (3) 3′tsRNA-Gly without any RNA modification. We compared their secondary structures and stability against RNase (Fig. 4d) on native PAGE gels, and observed that a lack of m5C at the C38 position (which represents the condition *Dnmt2*-/-) significantly changed the secondary RNA structure, and surprisingly increased stability against RNase degradation (Fig. 4d). These findings suggest that position-specific RNA modifications (m5C) can contribute greatly to the structural and biological properties of small RNAs. Moreover, by transfecting these synthesized small RNAs into NIH/3T3 cells, we found that the three types of 3′ tsRNA-Gly with different m5C modifications induced distinct transcriptomic responses at specific gene categories, including ribosome pathway-related gene clusters (Supplementary Fig. 4c). Such differences may reflect the effects of RNA secondary structural information induced by RNA modifications. This observation also relates to recent studies showing an intricate interplay between tsRNAs and ribosome function[32,33]. Together, these RNA modification-dependent effects provided further insights into how Dnmt2-mediated RNA modifications may impact the features of tsRNAs and thus their biological functions in the cell, although their direct effects on inheritance of the paternally acquired phenotype still awaits further studies. Nonetheless, our data suggest that differential RNA modifications harboured by sperm sncRNAs can increase their 'information capacity' beyond their linear sequence.

In summary, in addition to the recent emerging evidence of sperm RNA-mediated transmission of paternally acquired traits to offspring[2–5], the present work further identified *Dnmt2* as a genetic factor that is essential in shaping the sperm RNA 'coding signature'
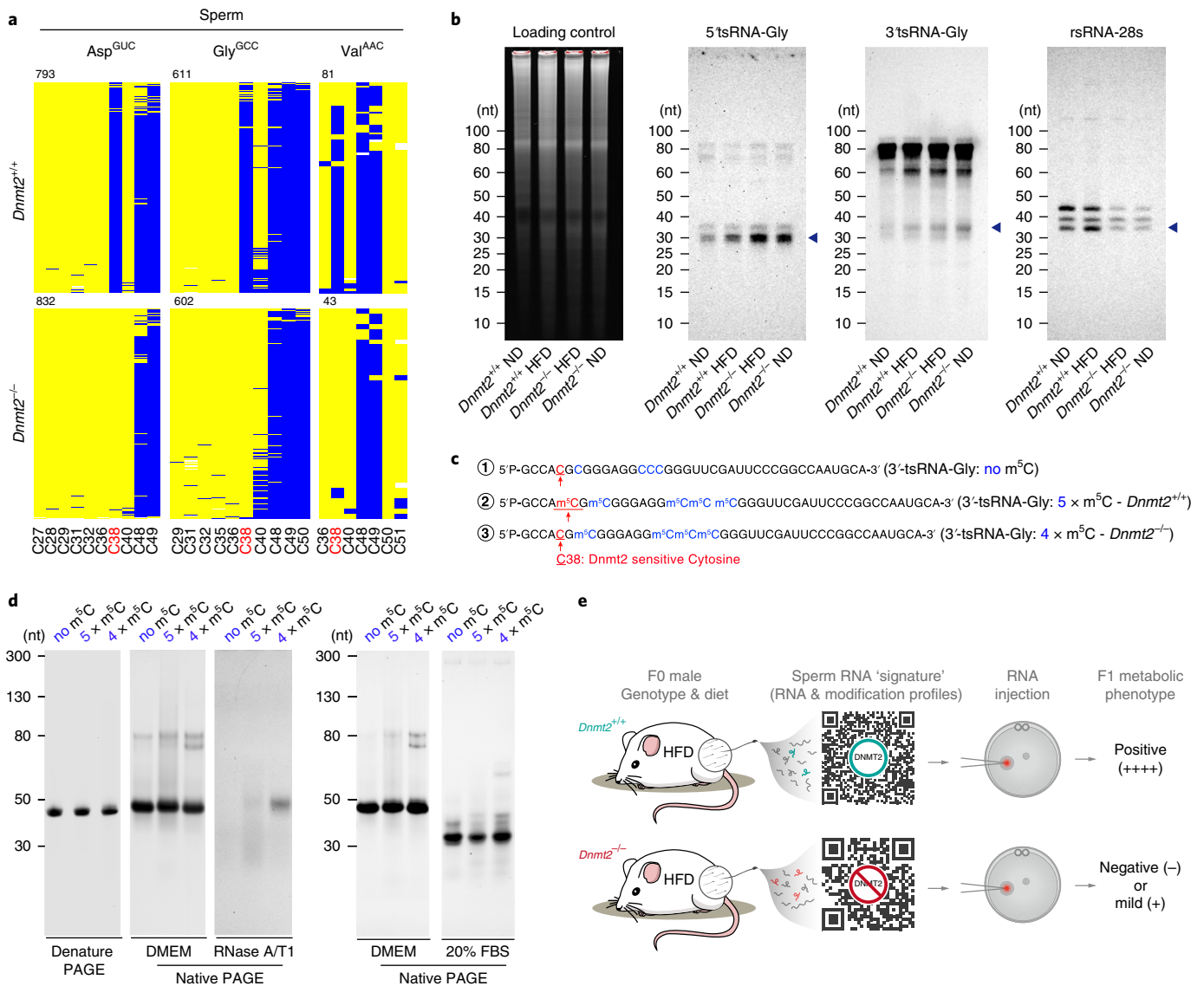
Fig. 4 | Dnmt2-dependent m⁵C modification regulates sperm tsRNA level and biological properties of tsRNA. a, Dnmt2-dependent C38 methylation in sperm. Bisulfite sequencing maps for the three known tRNA targets of DNMT2 (tRNA-Asp, tRNA-Gly and tRNA-Val) in mouse sperm (*Dnmt2*$^{+/+}$ and *Dnmt2*$^{-/-}$). Each row represents one sequence read, each column a cytosine residue. Yellow boxes represent unmethylated cytosine residues; blue boxes indicate methylated cytosine residues (m⁵C). Sequencing gaps are shown in white. Numbers above the maps indicate the number of reads. Cytosine C38 is labelled in red, and other cytosine sites in black. **b**, Northern blot analyses of 5′tsRNA-Gly, 3′tsRNA-Gly and rsRNA-28S (shown by arrow heads) in *Dnmt2*$^{+/+}$ ND, *Dnmt2*$^{+/+}$ HFD, *Dnmt2*$^{-/-}$ HFD and *Dnmt2*$^{-/-}$ ND sperm RNA. Sperm total RNAs extracted from two mice were mixed together for each lane in the experiment. Sperm total RNAs were run on a 15% denatured PAGE gel shown as a loading control. Blots are shown as representatives of three independent experiments (for rsRNA-28S) or two independent experiments (for tsRNAs) with similar results. **c**, Sequence of chemically synthesized 3′ tsRNA-Gly that harbours five m⁵C according to the *Dnmt2*$^{+/+}$ condition (5× m⁵C), 3′tsRNA-Gly with four m⁵C, lacking a Dnmt2-mediated m⁵C at the C38 position (4× m⁵C), and 3′tsRNA-Gly without any RNA modification (no m⁵C). **d**, Site-specific m⁵C alters the secondary structure of tsRNA, as well as the resilience against RNase degradation. In the native PAGE gel, it is shown that a lack of m⁵C at the C38 position (with four m⁵C) significantly changed the secondary structure of tsRNA, and that the tsRNA with four m⁵C is more resilient to RNase degradation than with no m⁵C or with five m⁵C, as tested by RNase A/T1 and 20% FBS (fetal bovine serum, which contains a unique combination of RNases). Each panel is representative of three independent experiments with similar results. **e**, Illustration of the essential role of DNMT2 in shaping the sperm RNA 'coding signature' (consisting of RNA expression and modification profiles) to confer intergenerational transmission of HFD-induced paternal metabolic disorders.

(consisting of a combination of RNA expression and modification profiles) that is responsible for the intergenerational transmission of HFD-induced paternal metabolic disorders (Fig. 4e). The effects of DNMT2 on sperm sncRNAs can in part be explained by its known enzyme activity, the loss of which causes hypomethylation of m⁵C and facilitates tRNA fragmentation[17,18] (Fig. 4a,b), and alter the chemical and biological properties of tsRNAs (Fig. 4c,d and Supplementary Fig. 4b,c). The Dnmt2-mediated sperm sncRNAs

profiles, along with the associated modifications, may also interact with large RNAs (mRNAs, lncRNAs, and so on) in the sperm or with RNAs that are encountered after fertilization, thus generating synergistic effects during early embryo development by regulating transcriptional cascades[4], transposon activities[6,34] and other potential regulatory pathways that eventually affect offspring phenotypes.

Data obtained from our present study also suggest that unidentified *Dnmt2* functions await to be discovered, particularly regard-

ing how *Dnmt2* may respond to paternal environmental clues (for example, diet variations) and encode such information into a sperm RNA signature. Further exploration of these mechanisms will lead to a deeper understanding of the 'information capacity' mediated by the versatile combinations of sperm RNAs and RNA modifications[35], and the circumstances under which a paternally acquired phenotype could be inherited by the offspring. These mechanisms could be highly relevant to human health because the structure and function of DNMT2 are highly conserved, and have been harnessed to respond to environmental challenges during evolution[15,36].

Methods

Methods, including statements of data availability and any associated accession codes and references, are available at https://doi.org/10.1038/s41556-018-0087-2.

References

1. Chen, Q., Yan, W. & Duan, E. Epigenetic inheritance of acquired traits through sperm RNAs and sperm RNA modifications. *Nat. Rev. Genet.* **17**, 733–743 (2016).
2. Gapp, K. et al. Implication of sperm RNAs in transgenerational inheritance of the effects of early trauma in mice. *Nat. Neurosci.* **17**, 667–669 (2014).
3. Rodgers, A. B., Morgan, C. P., Leu, N. A. & Bale, T. L. Transgenerational epigenetic programming via sperm microRNA recapitulates effects of paternal stress. *Proc. Natl Acad. Sci. USA* **112**, 13699–13704 (2015).
4. Chen, Q. et al. Sperm tsRNAs contribute to intergenerational inheritance of an acquired metabolic disorder. *Science* **351**, 397–400 (2016).
5. Grandjean, V. et al. RNA-mediated paternal heredity of diet-induced obesity and metabolic disorders. *Sci. Rep.* **5**, 18193 (2015).
6. Sharma, U. et al. Biogenesis and function of tRNA fragments during sperm maturation and fertilization in mammals. *Science* **351**, 391–396 (2016).
7. Miska, E. A. & Ferguson-Smith, A. C. Transgenerational inheritance: models and mechanisms of non-DNA sequence-based inheritance. *Science* **354**, 59–63 (2016).
8. Wei, Y. et al. Paternally induced transgenerational inheritance of susceptibility to diabetes in mammals. *Proc. Natl Acad. Sci. USA* **111**, 1873–1878 (2014).
9. Radford, E. J. et al. In utero effects. In utero undernourishment perturbs the adult sperm methylome and intergenerational metabolism. *Science* **345**, 1255903 (2014).
10. Siklenka, K. et al. Disruption of histone methylation in developing sperm impairs offspring health transgenerationally. *Science* **350**, aab2006 (2015).
11. Liebers, R., Rassoulzadegan, M. & Lyko, F. Epigenetic regulation by heritable RNA. *PLoS Genet.* **10**, e1004296 (2014).
12. Kiani, J. et al. RNA-mediated epigenetic heredity requires the cytosine methyltransferase Dnmt2. *PLoS Genet.* **9**, e1003498 (2013).
13. Nelson, V. R., Heaney, J. D., Tesar, P. J., Davidson, N. O. & Nadeau, J. H. Transgenerational epigenetic effects of the Apobec1 cytidine deaminase deficiency on testicular germ cell tumor susceptibility and embryonic viability. *Proc. Natl Acad. Sci. USA* **109**, 2766–2773 (2012).
14. Zhang, X., Cozen, A. E., Liu, Y., Chen, Q. & Lowe, T. M. Small RNA modifications: integral to function and disease. *Trends Mol. Med.* **22**, 1025–1034 (2016).
15. Lyko, F. The DNA methyltransferase family: a versatile toolkit for epigenetic regulation. *Nat. Rev. Genet.* **19**, 81–92 (2018).
16. Goll, M. G. et al. Methylation of tRNAAsp by the DNA methyltransferase homolog Dnmt2. *Science* **311**, 395–398 (2006).
17. Tuorto, F. et al. RNA cytosine methylation by Dnmt2 and NSun2 promotes tRNA stability and protein synthesis. *Nat. Struct. Mol. Biol.* **19**, 900–905 (2012).
18. Tuorto, F. et al. The tRNA methyltransferase Dnmt2 is required for accurate polypeptide synthesis during haematopoiesis. *EMBO J.* **34**, 2350–2362 (2015).
19. Peng, H. et al. A novel class of tRNA-derived small RNAs extremely enriched in mature mouse sperm. *Cell Res.* **22**, 1609–1612 (2012).
20. Holland, M. L. et al. Early-life nutrition modulates the epigenetic state of specific rDNA genetic variants in mice. *Science* **353**, 495–498 (2016).
21. Shea, J. M. et al. Genetic and epigenetic variation, but not diet, shape the sperm methylome. *Dev. Cell* **35**, 750–758 (2015).
22. Teh, A. L. et al. The effect of genotype and in utero environment on interindividual variation in neonate DNA methylomes. *Genome Res.* **24**, 1064–1074 (2014).
23. Wang, X. & Moazed, D. DNA sequence-dependent epigenetic inheritance of gene silencing and histone H3K9 methylation. *Science* **356**, 88–91 (2017).
24. Laprell, F., Finkl, K. & Muller, J. Propagation of polycomb-repressed chromatin requires sequence-specificrecruitment to DNA. *Science* **356**, 85–88 (2017).
25. Klosin, A., Casas, E., Hidalgo-Carcedo, C., Vavouri, T. & Lehner, B. Transgenerational transmission of environmental information in *C. elegans*. *Science* **356**, 320–323 (2017).
26. Ciabrelli, F. et al. Stable Polycomb-dependent transgenerational inheritance of chromatin states in *Drosophila*. *Nat. Genet.* **49**, 876–886 (2017).
27. Coleman, R. T. & Struhl, G. Causal role for inheritance of H3K27me3 in maintaining the OFF state of a Drosophila HOX gene. *Science* **356**, eaai8236 (2017).
28. Su, D. et al. Quantitative analysis of ribonucleoside modifications in tRNA by HPLC-coupled mass spectrometry. *Nat. Protoc.* **9**, 828–841 (2014).
29. Liu, F. et al. ALKBH1-mediated tRNA demethylation regulates translation. *Cell* **167**, 816–828 (2016).
30. Chu, C. et al. A sequence of 28S rRNA-derived small RNAs is enriched in mature sperm and various somatic tissues and possibly associates with inflammation. *J. Mol. Cell Biol.* **9**, 256–259 (2017).
31. Legrand, C. et al. Statistically robust methylation calling for whole-transcriptome bisulfite sequencing reveals distinct methylation patterns for mouse RNAs. *Genome Res.* **27**, 1589–1596 (2017).
32. Kim, H. K. et al. A transfer-RNA-derived small RNA regulates ribosome biogenesis. *Nature* **552**, 57–62 (2017).
33. Gebetsberger, J., Wyss, L., Mleczko, A. M., Reuther, J. & Polacek, N. A tRNA-derived fragment competes with mRNA for ribosome binding and regulates translation during stress. *RNA Biol.* **14**, 1364–1373 (2017).
34. Schorn, A. J., Gutbrod, M. J., LeBlanc, C. & Martienssen, R. LTR-retrotransposon control by tRNA-derived small RNAs. *Cell* **170**, 61–71 (2017).
35. Schimmel, P. The emerging complexity of the tRNA world: mammalian tRNAs beyond protein synthesis. *Nat. Rev. Mol. Cell Biol.* **19**, 45–58 (2018).
36. Jeltsch, A. et al. Mechanism and biological role of Dnmt2 in nucleic acid methylation. *RNA Biol.* **14**, 1108–1123 (2017).

Author contributions

Q.C., Y.F.Z. and Ying Z. conceived the idea and designed experiments. Q.C. and Y.F.Z. wrote the main manuscript and integrated inputs from all authors. Y.F.Z., X.Z. and Xin L. performed the mouse breeding, embryo manipulation related experiments and phenotype analyses, with help from Y.S.L., S.C.L., Y.C., X.H.L., L.Z., Y.Q., J.Q., Z.C., Y.W., H.L.Z., Ying Z., L.L. and under the supervision of Qi Z. and E.D. Y.F.Z., X.Z. and Ying Z. contributed to the RNA modifications analysis with help from Ying L., M.Y., Qiwei Z., R.W., D.Q. and under the supervision of Ying Z. and Q.C. Y.F.Z. prepared sperm RNA samples for next-generation sequencing with the help of H.Y.P., W.Y. and under the supervision of Ying Z. J.S. performed bioinformatics analyses for small RNA-seq and transcriptome data with help from T.Z., and the data were interpreted by J.S., Q.C. and T.Z. RNA modification and RNA secondary structure experiments were performed by Y.F.Z., M.P. and under the supervision of Q.C. Northern blot, bisulfite sequencing and Dnmt2 mice fertility analyses were performed by F.T. and Y.F.Z. with help from F.L., M.P. and R.L. X.Z. performed cell transfection experiments. Q.C. communicated with the editor and coordinated communications with Ying Z., Qi. Z., and E.D., who supervised different aspects of the paper.

Competing interests

The authors declare no competing interests.

Additional information

Supplementary information is available for this paper at https://doi.org/10.1038/s41556-018-0087-2.

Reprints and permissions information is available at www.nature.com/reprints.

Correspondence and requests for materials should be addressed to Y.Z. or Q.Z. or E.D. or Q.C.

Publisher's note: Springer Nature remains neutral with regard to jurisdictional claims in published maps and institutional affiliations.

Methods

Mice. Animal experiments were conducted under the protocol and approval of the Animal Care and Use Committee of the Institute of Zoology, Chinese Academy of Sciences, China, the Animal Care and Use Committee of the German Cancer Research Center, Heidelberg, Germany, and the Institutional Animal Care and Use Committee of the University of Nevada, Reno. The present study is compliant with all relevant ethical regulations regarding animal research. For experiments performed in China, Dnmt2 homozygote knockout mice were imported from The Jackson Laboratory (Dnmt2 KO, B6;129-Dnmt2tm1Bes/J) and were backcrossed for more than five generations into the C57BL/6NCrl genetic background (Charles River Laboratories China) before experiments were carried out (Supplementary Fig. 1c). Male *Dnmt2*^{+/+} and *Dnmt2*^{-/-} mice were housed in cages at a temperature of 22–24 °C and randomly divided into two diet groups for each genotype, one group received a high-fat diet (HFD, D12492; Research Diets) and the other group received a normal diet (Diet 1415, Beijing HFK Bioscience Co.). The recipient zygotes for microinjection of sperm total RNAs, sperm 30–40 nt RNAs and control injection were from mice with Institute of Cancer Research (ICR) backgrounds. For embryo transfer, all surrogate mothers had ICR background. All mice had access to food and water ad libitum and were maintained on a 12:12 h light–dark artificial lighting cycle, with lights off at 19:00. Alternatively, the Dnmt2 mouse line was held by the DKFZ animal facility. Those mice were used for sperm and testis northern blot analyses (Supplementary Fig. 1a) and bisulfite sequencing analyses (Fig. 4a and Supplementary Fig. 4a).

Sperm sample collection and RNA extraction. Mature sperm were isolated from the cauda epididymis and vas deferens of F0 fathers (*Dnmt2*^{+/+} HFD versus ND or *Dnmt2*^{-/-} HFD versus ND) and processed for RNA extraction as previously described[4].

Small RNA libraries construction. Small RNA libraries were constructed using TruSeq Small RNA Sample Prep Kit (Illumina). The small RNA libraries were prepared followed by library quality validation for sequencing. All RNA library preparation, quality examination and RNA sequencing were performed by BGI. We sequenced two biological repeats for sperm RNAs from *Dnmt2*^{+/+} HFD, *Dnmt2*^{+/+} ND, *Dnmt2*^{-/-} HFD and *Dnmt2*^{-/-} ND males. Each sample was prepared by pooling two mice sperm total RNAs.

Small RNA sequencing and quality control. For each RNA library, more than 10 million reads (raw data) were generated by Illumina Hi-Seq 2000. Sequence reads that fit any of the following parameters were removed with standard quality control criteria: (1) reads with *N* more than 4 bases whose quality score is lower than 10 or more than 6 bases whose quality score is lower than 13; (2) reads with 5′ primer contaminants or without 3′ primer; (3) reads without the insert tag; (4) reads with ploy A; (5) reads shorter than 18 nt. Clean reads were obtained after data filtration.

Small RNA-seq data processing and analysis. *Mapping strategy.* Small RNA sequences were mapped to each annotation database by Bowtie 1[37] to analyse their distribution and expression. The standard parameters used in Bowtie were '-v 0 -k 1'.

Small RNA annotation. Small RNA sequences were annotated using the pipeline SPORTS (Small non-coding RNA annotation Pipeline Optimized for rRNA- and tRNA-Derived Small RNAs, https://github.com/junchaoshi/sports1.0). The pipeline revealed many rRNA-derived small RNAs (rsRNAs) (Supplementary Fig. 3e-m) which were previously considered 'unmatch genome' or unannotated. One reason for this is that these rsRNAs derive from rRNA genes (rDNA) that are not properly assembled[38] and not shown in the mouse genome (mm10). The other reason is that previous non-coding RNA databases (for example, ensembl, Rfam) may not contain the complete rRNA sequences. We solved this problem by assembling a rRNA database by manually collect each rRNA sequences from NCBI and thus the rsRNAs from the RNA-seq data sets could be properly annotated. Expression levels were normalized to reads per million (RPM).

Isolation of RNAs of different sizes from sperm total RNAs. Total RNA was extracted from sperm using Trizol (Invitrogen, cat. no. 15596026) as described previously[4]. 1–2 μg total sperm RNA was separated on 15% PAGE with 7 M urea. The gel was stained with SYBR Gold Nucleic Acid Gel Stain (Invitrogen, cat. no. S11494). Small RNAs sized at 15–25, 30–40, 40–100 and >100 nt were excised from the gel and extracted as previously described[4]. The small RNAs extracted from the gel were then used for small RNA zygotic injection (30–40 nt) or alternatively used for RNA modification detection/quantification experiments (15–25, 30–40, 40–100 and >100 nt). For RNA modification quantification by LS-MS/MS, ~10 μg total sperm RNAs were needed in each group per experiment.

Zygote collection. Embryo collection and transfer were performed as previously described[4]. In brief, virgin female mice (ICR background) aged 6 weeks were selected as oocyte donors for superovulation, which was performed by intraperitoneal injection with 7.5IU PMSG (Prospec, cat. no. hor-272-a), after 48 h

intraperitoneal injection with hCG (Prospec, cat. no. hor-250-a). Zygotes were collected from the successfully mated female mouse.

Sperm RNAs microinjection and embryo transfer. Fertilization was confirmed by the presence of two pronuclei. Total sperm RNAs, or small RNAs isolated from total sperm RNAs with nucleotide length ranging from 30 to 40 nt, were adjusted to a concentration of 2 ng μl⁻¹ and microinjected into the male pronuclei of the ICR background fertilized eggs using a Nikon microinjection system. This amount approximately equals the total RNA of 10 sperm according to a previous report[4]. Injection of RNase free water into the male pronuclei of the ICR background fertilized eggs was performed as control. The zygotes were then cultured in M16 medium (Sigma, cat. no. M7292) at 37 °C in 5% CO_2. Two-cell embryos were transferred to the oviduct of a surrogate mother of ICR background. Each surrogate female received the embryo transfer in one side of the two oviducts, with 15–20 embryos for each transfer. A summary of the outcome after different types of RNA injection into normal zygotes is provided in Supplementary Table 2.

Blood glucose during GTT and ITT, and serum insulin examination during GTT. During GTT, an intraperitoneal injection of glucose as a single dose of 2 g per kg body weight was carried out in a 15 h fasted F0 HFD father, a 6 h fasted F0 ND father or microinjection F1 offspring. F0 males were tested at 6 months of age. For F1 male offspring, we performed the glucose GTT at age 16 weeks, glucose ITT at 17 weeks, and insulin level test during GTT at 18 weeks of age. The mice could rest and recover for one week between tests. For GTT experiments, blood samples were collected from the tail vein before glucose injection (0 min) and at 15, 30, 60 and 120 min afterward. The concentration of blood glucose was immediately measured using a glucose meter and test strips (ONETOUCH Ultra, LifeScan). The glucose value for each mouse at each time point was generated as the mean of two repeat measurements. For serum insulin measurements, collected blood was maintained at room temperature for 30 min, and centrifuged at 3,000*g* for 15 min at 4 °C for serum collection; serum samples were then processed for insulin concentration assays by ELISA (Millipore, cat. no. EZRMI-13K). Areas under the curve (AUCs) for blood glucose and insulin levels during the GTT were calculated using the trapezoidal rule.

ITTs were performed by intraperitoneal injection of insulin (0.75 IU kg⁻¹, Aladdin, CAS 12584-58-6, cat. no. I113907). The concentration of blood glucose was measured before insulin injection (0 min) and 30, 60, 90 and 120 min after insulin injection. Blood samples were collected the tail vein, and blood glucose concentrations were immediately measured with a glucose meter (ONETOUCH Ultra, LifeScan). The glucose value for each mouse at each time point was generated as the mean of two repeat measurements. AUCs for blood glucose during the ITT were calculated using the trapezoidal rule.

In Figs. 1b–h, 2 and Supplementary Fig. 2i-m, *n* represents the number of mice used in each group, depending on the availability of mice. The numbers of mice in each group were pooled from multiple experiments, and the numbers of experiments are detailed in the figure legends.

RT–PCR and quantitative RT–PCR. Total RNA was extracted from tissues using TRIzol reagent (Invitrogen, cat. no. 15596026) according to the manufacturer's instructions. Total RNA was processed to remove genome DNA using RQ1 RNase-Free DNase (Promega, cat. no. M6101). Then, 1 μg of RNA was reverse transcribed using the M-MuLV Reverse Transcriptase Reaction system (NEB, cat. no. M0253L). cDNAs obtained were diluted and used for quantitative PCR (qPCR). Each qPCR assay was performed with a standard dilution curve of a calibrator, for a mixture of different cDNA, to precisely quantify relative transcript levels. Gene-specific primers were used with SYBR green (Promega, cat. no. A6002) for detection on a LightCycler 480 system (Roche). The primer sequences used were synthesized by BGI as shown below:

dnmt2 primer-F: AGAAAGGGACAGGAAACA;
dnmt2 primer-R: CAATAACTTGGGTGGTAAA;
actin primer-F: TGGAATCCTGTGGCATCCATGAAAC;
actin primer-R: TAAAACGCAGCTCAGTAACAGTCCG.

Northern blots. RNA was extracted from testes and sperm and separated by 15% urea-PAGE. Gels were stained with SYBR Gold, and immediately imaged and transferred to Nytran SuperCharge membranes (Schleicher and Schuell, cat. no. 32-10416296), and UV crosslinked with an energy of 0.12 J. Membranes were pre-hybridized with DIG pre-hybridization (Roche: DIG Easy Hyb, REF: 11603558001) for at least 1 h at 42 °C. For detection of 5′tsRNA-Gly, 3′tsRNA-Gly and rsRNA-28s in mouse sperm RNA, membranes were incubated overnight (12–16 h) at 42 °C with DIG-labelled oligonucleotides probes synthesized by Integrated DNA Technologies (IDT) as follows:

5′-tsRNA-Gly: 5′-DIG-TCTACCACTGAACCACCAAT; 3′-tsRNA-Gly: 5′-DIG-ATTCCGGGAATCGAACCCGGGTCCT; rsRNA-28S: 5′-DIG-CGGGTCGCCACGTCTGATCTGAGGTCGCG.

Probes were added to the hybridization solution at a final concentration of 16 nM, and incubated overnight. The membranes were washed twice with low stringent buffer (2× SSC with 0.1% (wt/vol) SDS) at 42 °C for 15 min each,

then rinsed twice with high stringent buffer (0.1× SSC with 0.1% (wt/vol) SDS) for 5 min each, and then finally rinsed in washing buffer (1× SSC) for 10 min. Following the washes, the membranes were transferred into 1× blocking buffer (Roche REF:11096176001) and incubated at room temperature for 2–3 h, after which the DIG antibody (Roach: Anti-Digoxigenin-AP Fab fragments, REF: 11093274910) was added into the blocking buffer at a ratio of 1:10,000 and incubated for an additional half hour at room temperature. The membranes were then washed four times in DIG washing buffer (1× maleic acid buffer, 0.3% Tween-20) for 15 min each, rinsed in DIG detection buffer (0.1 M Tris-HCl, 0.1 M NaCl, pH 9.5) for 5 min, and then coated with CSPD ready-to-use reagent (Roach REF: 11755633001). The membranes were incubated in the dark with the CSPD reagent for 15 min at 37 °C before imaging using a Bio-Rad imaging system. (Fig. 4b)

For the ^{32}P-end-labelled oligonucleotides probe, the membranes were incubated overnight at 43–48 °C with the probes (Gly: TCTACCACTGAACCACCGAT; Asp: ACCACTATACTAACGAGGA; Glu: TTCCCTGACCGGGAATCGAACCC; Ser: CACTCGGCCCACCTCGTC) in hybridization solution (5× SSC, 20 mM Na$_2$HPO$_4$, pH 7.4, 7% SDS, 1× Denhardt's). Following overnight incubation, the membranes were washed for 15 min at 43 °C with 3× SSC, 5% SDS and for 15 min at room temperature with washing buffer (1× SSC, 1% SDS). Membranes were exposed on film, then stripped and re-hybridized for further analysis (Supplementary Fig. 1a).

RNA bisulfite sequencing. Testes were mechanically homogenized in TRIzol (Invitrogen, cat. no. 15596026) using a TissueRuptor (Qiagen). Sperm RNAs were prepared as previously mentioned. Bisulfite conversion was performed using the EZ RNA Methylation™ Kit (Zymo Research, cat. no. R5001) according to the manufacturer's protocol. Amplicons for 454 (Roche) sequencing were generated and analysed as described previously[17].

Ribonucleosides used as LC-MS/MS standards. 2′-O-methylguanosine (Gm, cat. no. PR3760), pseudouridine (Ψ, cat. no. PYA11080), 2′-O-methyluridine (Um, cat. no. PY 7690), 5,2′-O-dimethyluridine (m⁵Um, cat. no. PY7650), inosine (I, cat. no. 3725), 5-hydroxymethylcytidine (hm⁵C, cat. no. PY7596) and 3-methyluridine (m³U, cat. no. PY7694) were purchased from Berry & Associates. N4-acetylcytidine (ac⁴C, cat. no. NA05753), 1-methylguanosine (m¹G, cat. no. NM08574), N2-methylguanosine (m²G, cat. no. NM35522), N2,2,7-trimethylguanosine (m²,²,⁷G, cat. no. NT08918), N2,N2-dimethylguanosine (m²,²G, cat. no. ND05647) and 2′-O-methylinosine (Im, cat. no. ND05647) were purchased from Casrbosynth. Cytidine (C, cat. no. C4654), adenosine (A, cat. no. A9251), guanosine (G, cat. no. G6752), uridine (U, cat. no. U3750), 2′-O-methylcytidine (Cm, cat. no. M0259), 2′-O-methyladenosine (Am, cat. no. M9886), 5-methyladenosine (m⁵C, cat. no. M4254), 1-methyladenosine (m¹A, cat. no. M5001), 5-methyluridine (m⁵U, cat. no. 535893) and 7-methylguanosine (m⁷G, cat. no. M0627) were purchased from Sigma-Aldrich, N6-methyladenosine (m⁶A, cat. no. S3190) from SelleckChem, and [15N]5-2-deoxyadenosine ([15N]-dA, cat. no. NLM-3895) from Cambridge Isotope Laboratories.

LC-MS/MS-based RNA modification analysis for RNA samples. Standardized ribonucleosides preparation and mass spectrometry analysis were performed as previously described, with optimization[4,28]. Purified small RNAs (100–200 ng) from mice sperm were digested with 1 U benzonase nuclease (Sigma-Aldrich, cat. no. E8263), 0.05 U phosphodiesterase I (Affymetrix/USB, cat. no. J20240EXR) and 0.5 U alkaline phosphatase (Sigma-Aldrich, cat. no. P5521) in 37 °C for 3 h. Then, enzymes in the digestion mixture were removed via centrifugation using a Nanosep 3K device with Omega membrane (Sigma-Aldrich). Mass spectrometry analysis was performed on an Agilent 6460 Triple Quadrupole mass spectrometer connected to an Agilent 1200 HPLC system and equipped with an electrospray ionization source. The MS system was operated in positive ion mode using a multiple reaction monitoring (MRM) scan model. LC-MS/MS data were acquired by Agilent MassHunter Workstation Data Acquisition software, and processed by Agilent MassHunter Workstation Quantitative Analysis (version B.06) software for modified ribonuclosides concentration quantification. The percentage of each modified ribonucleoside was normalized to the total amount of quantified ribonucleosides with the same nucleobase, which decreases/eliminates errors caused by sample loading variation. For example, the percentage of m⁵C = mole concentration (m⁵C)/mole concentration (m⁵C + Cm + C + ac⁴C). The fold changes of RNA modifications between different groups were calculated based on the percentage of modified ribonuclosides. We examined the sperm RNAs with 15–25 and 30–40 nt as a priority, and in the middle of the project we added two groups (40–100 nt, >100 nt) to subsequent tests. Thus, there are larger n numbers in the groups of 15–25 and 30–40 nt RNAs than in the 40–100 and >100 nt RNAs.

Synthesis of tsRNAs with RNA modifications, examination of RNA secondary structure and RNA stability in native gels. RNAs modified with m⁵C were synthesized by GE Dharmacon and dissolved into DNase/RNase-free water at a concentration of 100 μM (Fig. 4d). RNAs were incubated at 37 °C for 15 min in DMEM-base systems: 5 μM RNAs in DMEM, or DMEM with 20% serum (FBS,

Thermo Fisher cat. no. 10099141), or DMEM with 0.1 μl RNase A/T1 (2 mg ml⁻¹ of RNase A and 5,000 U ml⁻¹ of RNase T1) Following incubation, the samples were immediately placed on ice, and 10× RNA native gel loading buffer (Ambio, cat. no. AM8556) was added. Prepared samples (1 μl) were loaded into the wells of 15% native PAGE gel, run at 4 °C. The gels were stained with SYBR Gold (Invitrogen, cat. no. S11494) before imaging.

Transfection of synthesized tsRNAs into cell line. We seeded 5×10^5 NIH/3T3 cells (ATCC CRL-1658) per well into the 12-well plate the day before transfection and waited until the cells reached 70–90% confluence at transfection. For a single-well transfection, 9 μl Lipofectamine 3000 reagent (Invitrogen, cat. no. L3000008) was diluted in 86 μl Opti-MEM medium (Invitrogen, cat. no. 31985062), to which was added 5 μl of 10 μM synthetic tsRNAs (Supplementary Fig. 4b). This was vortexed briefly and incubated for 15 min at room temperature to form the transfection complex. The culture medium was discarded, then 400 μl fresh culture medium was added to the cells. RNA-lipid transfection complex (100 μl) was added to each well for transfection. The final RNA concentration for transfection was 100 nM. The control group was composed of 9 μl Lipofectamine 3000 reagent and 86 μl Opti-MEM and 5 μl water without synthetic tsRNAs. After 4.5 h of transfection, the culture medium containing transfection complex was discarded, and the complex was transferred into new fresh culture medium. The cell total RNA was collected by Trizol reagent according to the manufacturer's instructions 12 h after transfection. RNA samples were then processed for library construction and RNA-seq.

mRNA library construction, RNA sequencing and quality control. Transcriptome libraries were constructed using the TruSeq Stranded mRNA Library Prep Kit (Illumina). For each RNA library, 4G base pairs (raw data) were generated by Illumina Hi-Seq 4000. After base composition and quality tests were passed, we removed the adapter sequence, where there was a high content of unknown bases (unknown bases comprised more than 5%) and low-quality reads. The clean reads were used for downstream bioinformatics analysis. All mRNA library preparation, quality examination and RNA sequencing were performed by Novogene.

Transcriptome data processing and analysis. *RNA annotation.* RNA sequences were annotated using kallisto[39] with Ensembl mouse cDNA annotation information (GRCm38). The expression level of each gene was normalized to TPM (transcripts per kilobase million).

Geneset score. The Functional Analysis of Individual Microarray Expression (FAIME) algorithm[40] was applied to assign a geneset score for the candidate Kyoto Encyclopedia of Genes and Genomes (KEGG) pathways. FAIME computes geneset scores using rank-weighted gene expression of individual samples, which converts each sample's transcriptomic information to molecular mechanisms[40]. Higher geneset scores indicate overall upregulation of a given KEGG pathway (Supplementary Fig. 4c).

Statistics and reproducibility. GraphPad Prism 7 was used to analyse data for mouse body weight, GTT, ITT, qPCR and levels of RNA modification. Data are presented as mean ± s.e.m., and $P < 0.05$ was considered statistically significant. Data were analysed by two-way ANOVA with uncorrected Fisher's LSD for Figs. 1c–e and 2b–d,f–h and Supplementary Fig. 1j,l, by one-way ANOVA with uncorrected Fisher's LSD for Figs. 1b,f–h, 2a,e,i–n and 3 and Supplementary Fig. 2, or by two-tailed unpaired Student's t-test for Supplementary Figs. 1b and 2i,k,m.

We performed resampling tests to understand the robustness of our statistical results. For each round of resampling, we randomly picked up samples from individual groups. Two-way ANOVA was conducted based on the subset of the original samples (data of $Dnmt2^{+/+}$ HFD versus $Dnmt2^{-/-}$ HFD from Fig. 2f) with reduced sample size. 1,000 resamplings were performed to obtain empirical P-value distributions as shown in Supplementary Fig. 1f,g, demonstrating the robustness of our statistical data.

All glucose values in Figs. 1b–h and 2 and Supplementary Fig. 1i–m were generated as the means of two repeat measurements for each mouse at each time point. n represents the number of mice used in each group, depending on the availability of mice. The number of mice in each group was pooled from multiple experiments, and the number of experiments are detailed in the figure legends. For the RNA LC-MS/MS experiment in Fig. 3 and Supplementary Fig. 2, three independent biological repeats were performed for 40–100 and >100 nt sperm RNA fractions. For 15–25 and 30–40 nt sperm RNA fractions, five to six repeats were performed (n is shown as individual dots in the figures, as detailed in Supplementary Table 1). Northern blots in Fig. 4b are representative of three independent experiments (for rsRNA-28S) or two independent experiments (for tsRNAs) with similar results. RNA PAGE gel results in Fig. 4d are representative of three independent experiments with similar results. Northern blots in Supplementary Fig. 1a are representative of two independent experiments with similar results. Two independent sets of sperm RNA samples were used for small RNA sequencing (Supplementary Fig. 3). Two sets of RNA samples were used for transcriptome sequencing (Supplementary Fig. 4c).

Reporting Summary. Further information on experimental design is available in the Nature Research Reporting Summary linked to this article.

Data availability. Small RNA-seq and transcriptome sequencing data that support the findings of this study have been deposited in the Gene Expression Omnibus (GEO) under accession code GSE97645. LC-MS/MS data have been deposited in Figshare (https://figshare.com/articles/_/5946373). Statistic source data for Fig. 1b–h, Fig. 2, Fig. 3 and Supplementary Fig. 1b,f,g,i–m, Supplementary Fig. 2 are provided in Supplementary Table 1. Uncropped blots and gels are provided in Supplementary Fig. 5. All other data supporting the findings of this study are available from the corresponding author on reasonable request.

References

37. Langmead, B., Trapnell, C., Pop, M. & Salzberg, S. L. Ultrafast and memory-efficient alignment of short DNA sequences to the human genome. *Genome Biol.* **10**, R25 (2009).
38. McStay, B. & Grummt, I. The epigenetics of rRNA genes: from molecular to chromosome biology. *Annu. Rev. Cell Dev. Biol.* **24**, 131–157 (2008).
39. Bray, N. L., Pimentel, H., Melsted, P. & Pachter, L. Near-optimal probabilistic RNA-seq quantification. *Nat. Biotechnol.* **34**, 525–527 (2016).
40. Yang, X. et al. Single sample expression-anchored mechanisms predict survival in head and neck cancer. *PLoS Comput. Biol.* **8**, e1002350 (2012).

Corresponding author(s):   Ying Zhang, Qi Zhou, Enkui Duan, Qi Chen

Reporting Summary

Nature Research wishes to improve the reproducibility of the work that we publish. This form provides structure for consistency and transparency in reporting. For further information on Nature Research policies, see Authors & Referees and the Editorial Policy Checklist.

Statistical parameters

When statistical analyses are reported, confirm that the following items are present in the relevant location (e.g. figure legend, table legend, main text, or Methods section).

n/a	Confirmed	
☐	☒	The exact sample size (*n*) for each experimental group/condition, given as a discrete number and unit of measurement
☐	☒	An indication of whether measurements were taken from distinct samples or whether the same sample was measured repeatedly
☐	☒	The statistical test(s) used AND whether they are one- or two-sided *Only common tests should be described solely by name; describe more complex techniques in the Methods section.*
☒	☐	A description of all covariates tested
☒	☐	A description of any assumptions or corrections, such as tests of normality and adjustment for multiple comparisons
☐	☒	A full description of the statistics including central tendency (e.g. means) or other basic estimates (e.g. regression coefficient) AND variation (e.g. standard deviation) or associated estimates of uncertainty (e.g. confidence intervals)
☐	☒	For null hypothesis testing, the test statistic (e.g. F, t, r) with confidence intervals, effect sizes, degrees of freedom and P value noted *Give P values as exact values whenever suitable.*
☒	☐	For Bayesian analysis, information on the choice of priors and Markov chain Monte Carlo settings
☒	☐	For hierarchical and complex designs, identification of the appropriate level for tests and full reporting of outcomes
☐	☒	Estimates of effect sizes (e.g. Cohen's *d*, Pearson's *r*), indicating how they were calculated
☐	☒	Clearly defined error bars *State explicitly what error bars represent (e.g. SD, SE, CI)*

Our web collection on statistics for biologists may be useful.

Software and code

Policy information about availability of computer code

Data collection	EXCEL 2016, MassHunter Quantitative Analysis Software B.06.00 Build 388.0
Data analysis	Graphpad prism 7, SPORTS1.0, kallisto, FAIME

For manuscripts utilizing custom algorithms or software that are central to the research but not yet described in published literature, software must be made available to editors/reviewers upon request. We strongly encourage code deposition in a community repository (e.g. GitHub). See the Nature Research guidelines for submitting code & software for further information.

Data

Policy information about availability of data

All manuscripts must include a data availability statement. This statement should provide the following information, where applicable:

- Accession codes, unique identifiers, or web links for publicly available datasets
- A list of figures that have associated raw data
- A description of any restrictions on data availability

Small RNA–seq and transcriptome sequencing data that support the findings of this study have been deposited in the Gene Expression Omnibus (GEO) under accession codes GSE97645. LC-MS/MS data have been deposited in Figshare (https://figshare.com/articles/_/5946373). Statistic source data for Fig. 1b-h, Fig. 2,

Fig.3 and Supplementary Fig. 1b,f,g,i-m, Supplementary Fig. 2 have been provided in Supplementary Table 1. Uncropped blots and gels are provided in Supplementary Fig.5. All other data supporting the findings of this study are available from the corresponding author on reasonable request.

Field-specific reporting

Please select the best fit for your research. If you are not sure, read the appropriate sections before making your selection.

☒ Life sciences   ☐ Behavioural & social sciences

For a reference copy of the document with all sections, see nature.com/authors/policies/ReportingSummary-flat.pdf

Life sciences

Study design

All studies must disclose on these points even when the disclosure is negative.

Sample size	The minimal sample size was decided based on power analysis of samples of our previous publications on the same project (Science. 2016 Jan 22;351(6271):397-400.) as well as the preliminary data we got from the present project to ensure a statistical power at the level (1-β) of 80% and a significance level (α) of 5% for t-test.
Data exclusions	For RNA modification quantification in Fig.3 and Supplementary Fig.2. During the analysis of the mass spectrometry data, we excluded data points when the signal peak is not in good quality (e.g. abnormal peaks, elevated baseline), or drifting off the detection time predetermined by each standardized ribonucleoside, which resulted in inaccurate reading (or loss of reading) of the examined signal. These situations are unpredictable and inevitable when performing high-throughput LS-MS/MS for multiple samples, mostly due to the intrinsic hardware environment of the machine. This might be also in part, due the relative low amount of RNAs available from sperm that were loaded for the experiment. The excluded original data is also provided, with a blue* mark in the source data shown in Supplementary Table 1.
Replication	All glucose value in Fig. 1b-h, Fig. 2 and Supplementary Fig. 1i-m was generated as the mean of two repeat measurements for each mouse at each time point. n numbers represent the mice used in each group, depending on the availability of mice. The number of mice in each group were pooled from multiple experiments. In Fig.1b-d,f,g and Fig.2d,g,h,k,m,n, data pooled from 7 experiments. In Fig.1e,h, data pooled from 4 experiments. In Fig.2a,b,e,f,i,l, data pooled from 10 experiments. In Fig.2c,j, data pooled from 8 experiments. In Supplementary Fig.2 i-m, data pooled from 2 experiments. For RNA LC-MS/MS experiment in Fig. 3 and Supplementary Fig. 2, three independent biological repeat were performed for 40-100nt and >100nt sperm RNA fractions. For 15-25nt and 30-40nt sperm RNA fractions, 5-6 repeats were performed (n numbers were shown as individual dots on the figures, and detailed in Supplementary Table 1). Two independent biological repeats were performed for each sperm small RNA-seq in Supplementary Fig. 3. Two independent biological repeats were performed for transcriptome sequencing in supplementary Fig. 4c. Northern blot in Fig.4b are shown as representatives of three independent experiments (for rsRNA-28S) or two independent experiments (for tsRNAs) with similar results. RNA PAGE gel results in Fig.4d are showed as representative of three independent experiments with similar results. Northern blot in Supplementary Fig.1a are shown as representatives of two independent experiments with similar results.
Randomization	F0 mice were randomly allocated into two groups to receive HFD or ND. A pool of normal zygotes were randomly assigned for different groups sperm RNA injection or control injection (water) experiments. No specific method of randomization was used.
Blinding	The genotypes of F0 mice and the diet conditions were known to the investigators at the outset of the study. Due to the obvious phenotype between F0 HFD and F0 ND males at 6 months of age, blinding to these two experimental conditions was challenging. F1 mice were generated by injecting different groups of sperm RNAs into zygotes, followed by embryo transfer into surrogate mother and allocated into different cages, these processes made it impossible to be blinded to the investigators.

Materials & experimental systems

Policy information about availability of materials

n/a	Involved in the study
☒	☐ Unique materials
☐	☒ Antibodies
☐	☒ Eukaryotic cell lines
☐	☒ Research animals
☒	☐ Human research participants

Antibodies

Antibodies used	Anti-Digoxigenin-AP Fab fragments (Roach, REF: 11093274910) used in the Northern blot experiments in Fig.4b is diluted in 1:10000.
Validation	The polyclonal antibody from sheep is specific to digoxigenin and digoxin and shows no cross-reactivity with other steroids, such as human estrogens and androgens. This antibody is validated and extensively use in previous publications, the weblink below shows that this antibody has been used in 145 peer-reviewd papers: https://www.sigmaaldrich.com/catalog/product/roche/11093274910?lang=en&region=US

Eukaryotic cell lines

Policy information about cell lines

Cell line source(s)	NIH/3T3 cells were obtained from the American Type Culture Collection(ATCC® CRL-1658)
Authentication	Cell line authentication were performed by ACTT using COI assay.
Mycoplasma contamination	The cell line has been tested negative for mycoplasma contamination
Commonly misidentified lines (See ICLAC register)	No cell lines used in this study were found in the database of commonly misidentified cell lines that is maintained by ICLAC and NCBI Biosample.

Research animals

Policy information about studies involving animals; ARRIVE guidelines recommended for reporting animal research

| Animals/animal-derived materials | Dnmt2 homozygous knock out mice (Dnmt2 KO, B6;129-Dnmt2tm1Bes/J) were imported from The Jackson Laboratory and were back-crossed for more than five generations into the C57BL/6NCrl genetic background (Charles River Laboratories China Inc) before experiments were carried out, the detailed breeding strategies are provided in Supplementary Fig. 1c. F0 male mice at the age of 6 months (fed with normal diet vs high-fat diet) were used for metabolic parameter tests and sperm RNA extraction.

For F0 males at the age of 6 months (Fig. 1b-h)
Dnmt2+/+ HFD F0 (mean weight: 47.31; weight range: 42.4-54.4, n=33; glucose GTT, n=33; glucose ITT, n=28; insulin GTT, n=8),
Dnmt2-/- HFD F0 (mean weight: 46.82; weight range: 38.7-56.6 n=33; glucose GTT, n=33; glucose ITT, n=28; insulin GTT, n=8),
Dnmt2+/+ ND F0 (mean weight: 33.53; weight range: 29.6-38.9 n=16; glucose GTT, n=16; glucose ITT, n=16; insulin GTT, n=8),
Dnmt2-/- ND F0 (mean weight: 30.54; weight range: 24.5-44.0 n=28; glucose GTT, n=15; glucose ITT, n=15; insulin GTT, n=8).

Sperm RNAs were used for zygotic micro-injection to generate the F1 offspring, RNA modification examination, northern blot in Fig.4b and small RNA sequencing. C57BL/6NCrl mice testes, caput epididymis, and cauda epididymis were collected for RNA extraction and qPCR analyses provided Supplemental Fig.1b. The surrogate mother and the recipient zygotes for micro-injection of sperm total RNAs, sperm 30-40nt RNAs and control injection were from mice of ICR backgrounds. F1 male offspring generated from RNA injection or naturally breeding were used for metabolic parameter tests.

For F1 males from sperm total RNA injection (Fig. 2a-d, i-k):
Dnmt2+/+ HFD sperm total RNA F1 (mean weight: 42.12; weight range: 32.40-51.85 at the age of 16 weeks, n=40; glucose GTT at the age of 16 weeks, n=37; glucose ITT at the age of 17 weeks, n=29; insulin GTT at the age of 18 weeks, n=14),
Dnmt2-/- HFD sperm total RNA F1 (mean weight: 40.56; weight range: 30.90-49.00 at the age of 16 weeks, n=27; glucose GTT at the age of 16 weeks, n=24; glucose ITT at the age of 17 weeks, n=24; insulin GTT at the age of 18 weeks, n=16),
Dnmt2+/+ ND sperm total RNA F1 (mean weight: 39.57; weight range: 32.98-47.40 at the age of 16 weeks, n=28; glucose GTT at the age of 16 weeks, n=27; glucose ITT at the age of 17 weeks, n=23; insulin GTT at the age of 18 weeks, n=9),
Dnmt2-/- ND sperm total RNA F1 (mean weight: 39.22; weight range: 35.00-45.80 at the age of 16 weeks, n=28; glucose GTT at the age of 16 weeks, n=28; glucose ITT at the age of 17 weeks, n=17; insulin GTT at the age of 18 weeks, n=8),
Control injection F1 (mean weight: 40.04; weight range: 30.90-47.30 at the age of 16 weeks, n=18; glucose GTT at the age of 16 weeks, n=18; glucose ITT at the age of 17 weeks, n=18; insulin GTT at the age of 18 weeks, n=8).

For F1 males from sperm 30-40nt RNA injection (Fig. 2e-h, l-n):
Dnmt2+/+ HFD sperm 30-40nt RNA F1 (mean weight: 39.47; weight range: 35.24-44.50 at the age of 16 weeks, n=42; glucose GTT at the age of 16 weeks, n=42; glucose ITT at the age of 17 weeks, n=18; insulin GTT at the age of 18 weeks, n=16),
Dnmt2-/- HFD sperm 30-40nt RNA F1 (mean weight: 39.36; weight range: 29.10-49.90 at the age of 16 weeks, n=52; glucose GTT at the age of 16 weeks, n=52; glucose ITT at the age of 17 weeks, n=30; insulin GTT at the age of 18 weeks, n=16),
Dnmt2+/+ ND sperm 30-40nt RNA F1 (mean weight: 40.26; weight range: 35.11-48.70 at the age of 16 weeks, n=18; glucose GTT at the age of 16 weeks, n=18; glucose ITT at the age of 17 weeks, n=18; insulin GTT at the age of 18 weeks, |

n=9),
Dnmt2-/- ND sperm 30-40nt RNA F1 (mean weight: 38.19; weight range: 29.30-48.25 at the age of 16 weeks, n=17; glucose GTT at the age of 16 weeks, n=17; glucose ITT at the age of 17 weeks, n=15; insulin GTT at the age of 18 weeks, n=8),
Control injection F1 (mean weight: 40.04; weight range: 30.90-47.30 at the age of 16 weeks, n=18; glucose GTT at the age of 16 weeks, n=18; glucose ITT at the age of 17 weeks, n=18; insulin GTT at the age of 18 weeks, n=8).

For F1 males generated by breeding Dnmt2-/- male (fed on ND or HFD) with Dnmt2-/- female mice (fed on ND) (Supplementary Fig. 1i-m)
Dnmt2-/- F1 from HFD father: (mean weight: 24.32; weight range: 22.70-26.40 at the age of 7 weeks, n=7; glucose GTT at the age of 7 weeks, n=7; glucose ITT at the age of 17 weeks, n=6),
Dnmt2-/- F1 from ND father: (mean weight: 21.71; weight range: 17.77-24.56 at the age of 7 weeks, n=10; glucose GTT at the age of 7 weeks, n=10; glucose ITT at the age of 17 weeks, n=5).

Alternatively, adult male Dnmt2+/+ and Dnmt2-/- mouse line held by the DKFZ animal facility were used for sperm and testis Northern Blot analysis (Supplementary Fig. 1a) and RNA bisulfite-sequencing analysis (Fig.4a and Supplementary Fig. 4a).

Method-specific reporting

n/a	Involved in the study
☒ ☐	ChIP-seq
☒ ☐	Flow cytometry
☒ ☐	Magnetic resonance imaging

In the format provided by the authors and unedited.

Dnmt2 mediates intergenerational transmission of paternally acquired metabolic disorders through sperm small non-coding RNAs

Yunfang Zhang [1,2,3,8], Xudong Zhang [2,8], Junchao Shi [2,8], Francesca Tuorto [4,8], Xin Li [1,8], Yusheng Liu[1], Reinhard Liebers[4], Liwen Zhang[1,3], Yongcun Qu[1,3], Jingjing Qian[1,3], Maya Pahima[2], Ying Liu[2], Menghong Yan[5], Zhonghong Cao[1,6], Xiaohua Lei[1], Yujing Cao[1], Hongying Peng[2], Shichao Liu[2], Yue Wang[2], Huili Zheng[2], Rebekah Woolsey[7], David Quilici[7], Qiwei Zhai[5], Lei Li [1], Tong Zhou[2], Wei Yan[2], Frank Lyko [4], Ying Zhang [1]*, Qi Zhou [1]*, Enkui Duan [1]* and Qi Chen [2]*

[1]State Key Laboratory of Stem Cell and Reproductive Biology, Institute of Zoology, Chinese Academy of Sciences, Beijing, China. [2]Department of Physiology and Cell Biology, University of Nevada, Reno School of Medicine, Reno, NV, USA. [3]University of Chinese Academy of Sciences, Beijing, China. [4]Division of Epigenetics, DKFZ-ZMBH Alliance, German Cancer Research Center, Heidelberg, Germany. [5]Key Laboratory of Nutrition and Metabolism, Chinese Academy of Sciences Center for Excellence in Molecular Cell Science, Institute for Nutritional Sciences, Shanghai Institutes for Biological Sciences, Chinese Academy of Sciences, Shanghai, China. [6]College of Life Sciences, Shandong University of Technology, Zibo, China. [7]Nevada Proteomics Center, University of Nevada, Reno School of Medicine, Reno, NV, USA. [8]These authors contributed equally: Yunfang Zhang, Xudong Zhang, Junchao Shi, Francesca Tuorto, Xin Li. *e-mail: zhangying@ioz.ac.cn; qzhou@ioz.ac.cn; duane@ioz.ac.cn; cqi@med.unr.edu
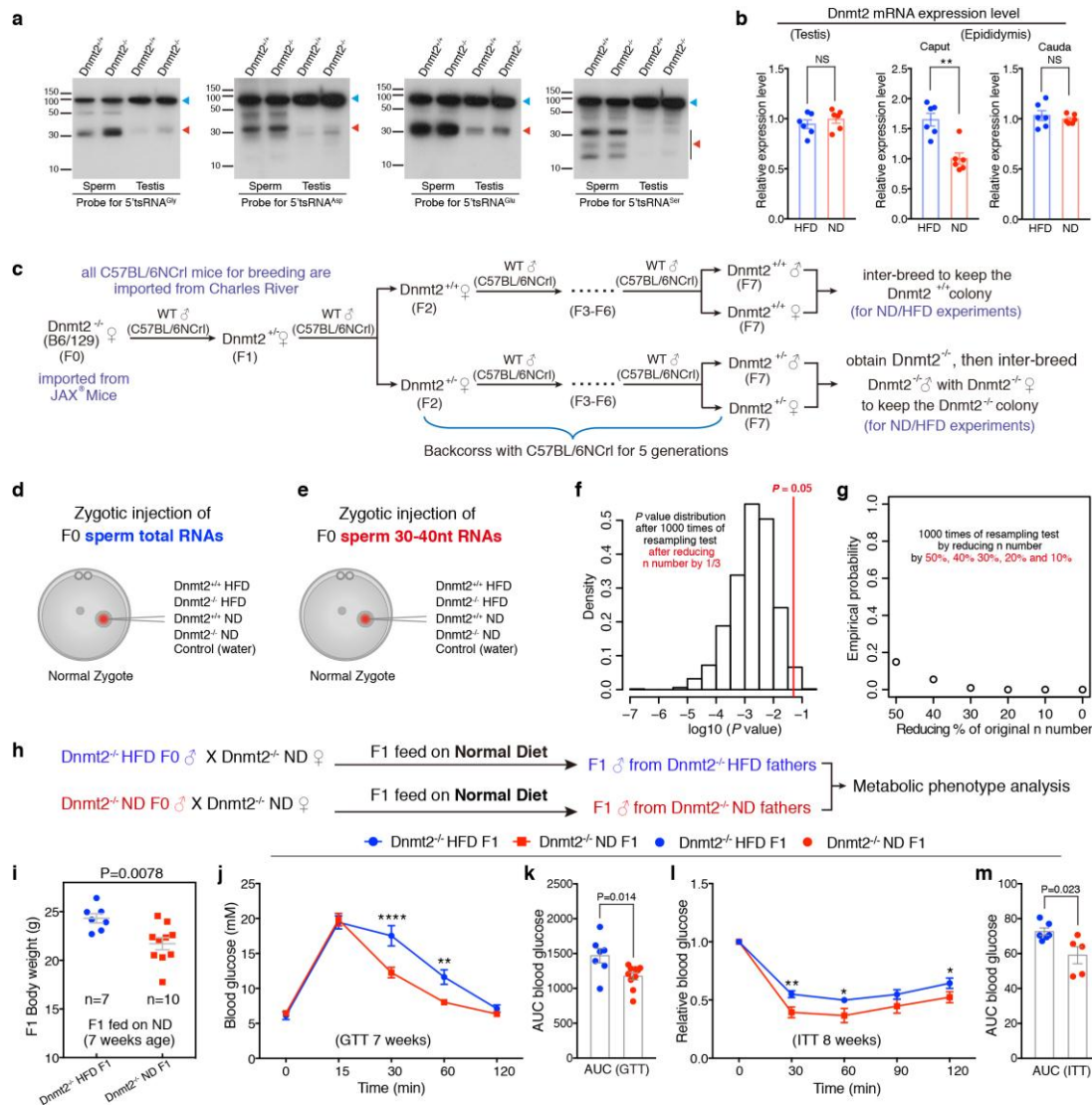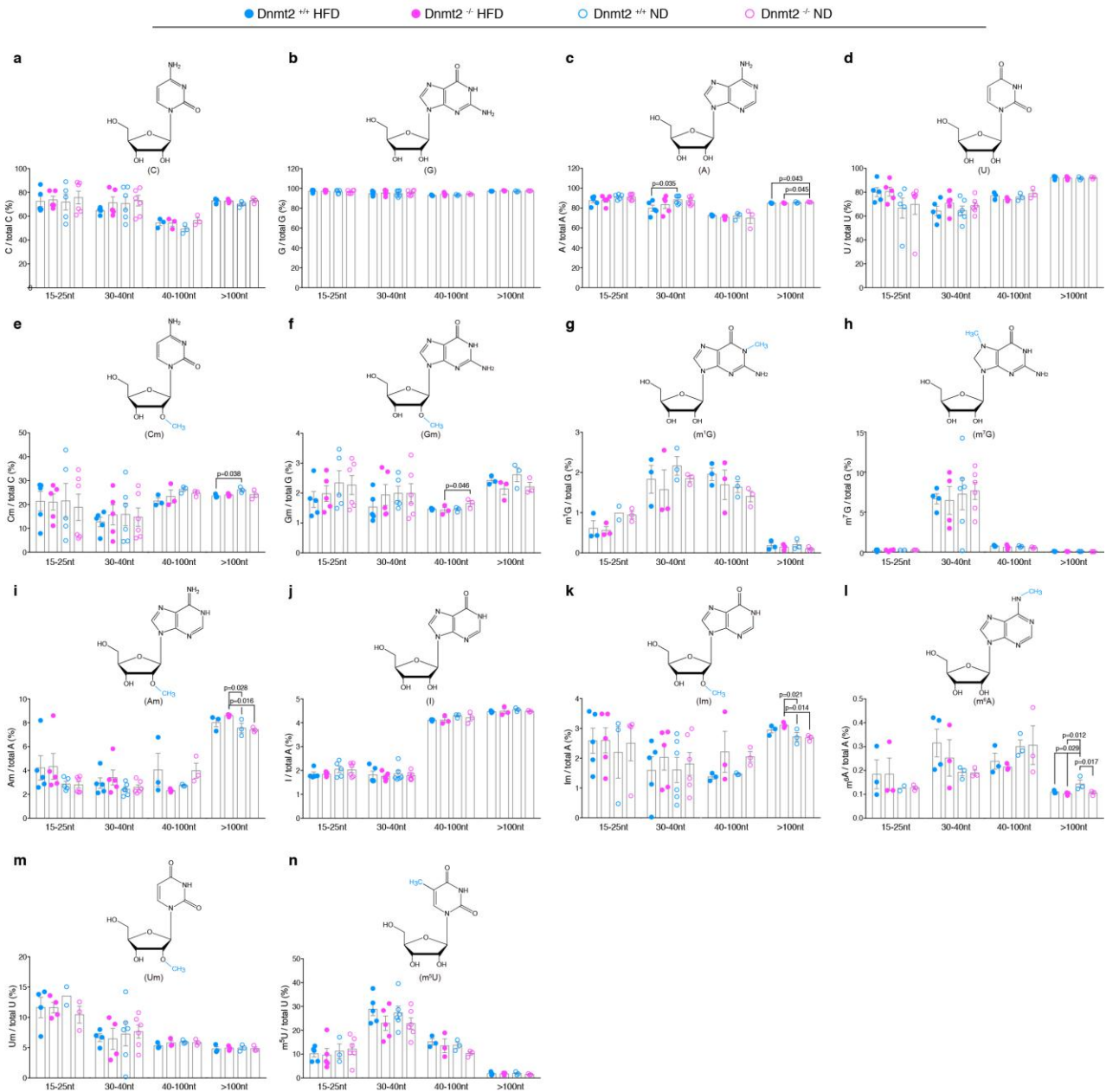
Supplementary Figure 1

Expression of tsRNAs and Dnmt2, breeding strategies and the metabolic parameters of F1 males generated by Dnmt2$^{-/-}$ mice breeding.

(a) Northern blot for tRNAs and tsRNAs in sperm and testis from *Dnmt2$^{+/+}$* and *Dnmt2$^{-/-}$* mice. Blue arrows indicate tRNAs, Red arrows indicate tsRNAs. Blots are shown as representatives of two independent experiments with similar results. **(b)** The relative expression level of Dnmt2 mRNA in mouse testis, caput epididymis and cauda epididymis under HFD or ND condition. Each dot represents one biologically independent experiment, n=6 biologically independent experiment. **P < 0.01, NS: not significant. **(c)** Breeding strategy to generate *Dnmt2$^{+/+}$* and *Dnmt2$^{+/+}$* F0 mice for experiments in **Figure.1**. **(d,e)** Illustration of zygotic injection of sperm **(d)** total RNAs, **(e)** 30-40nt RNAs and injection of water as control to generate F1 male offspring for phenotypic examination in **Figure.2**. **(f,g)** Representative resampling test between *Dnmt2$^{+/+}$* HFD vs *Dnmt2$^{-/-}$* HFD in **Figure.2f,** which were performed by reducing the n number of both groups by 1/3 **(f)**, or by 10-50% **(g)**, demonstrating the robustness of statistical significant difference between these two groups. **(h)** Mating strategy to generate F1 male for phenotypic analyses in **(i-m)**. **(i)** Body weights of F1 male fed on ND. Each dot represents one mouse, data pooled from 2 experiments. **(j)** Blood glucose of F1 male during the GTT. n=7 mice for F1 male generated from *Dnmt2$^{-/-}$* HFD group, and n=10 mice for F1 male generated from *Dnmt2$^{-/-}$* ND group; data pooled from 2 GTT experiments. **P < 0.01, ****P < 0.0001. **(k)** Area under the curve (AUC) statistics for GTT in **(j)**. **(l)** Relative blood glucose of F1 male during the ITT. n=6 mice for F1 male generated from *Dnmt2$^{-/-}$* HFD group, and n=5 mice for F1 male generated from *Dnmt2$^{-/-}$* ND group; data pooled from 2 ITT experiments. *P < 0.05, **P < 0.01 **(m)** AUC statistics for ITT in **(l).** All data are plotted as mean±SEM. Statistical analysis for **(b,l,k,m)** are performed by two-tailed unpaired Student's t-test, and **(j,l)** are performed by two-tailed, two-way Anova, uncorrected Fisher's LSD. All statistic source data and P values are provided in **Supplementary Table 1.**

Supplementary Figure 2

The level of different type of RNA modifications in sperm RNA fractions extracted from F0 *Dnmt2*$^{+/+}$ and *Dnmt2*$^{-/-}$ males under ND and HFD.

The relative level of unmodified **(a)** C, **(b)** G, **(c)** A, **(d)** U in different sperm RNA fractions (15-25nt, 30-40nt, 40-100nt and >100 nt and the relative level of modified nucleotide in **(e)** Cm, **(f)** Gm, **(g)** m^{1}G, **(h)** m^{7}G, **(i)** Am, **(j)** I, **(k)** Im, **(l)** m^{6}A, **(m)** Um, **(n)** m^{5}U from different sperm RNA fractions (15-25nt, 30-40nt, 40-100nt and >100 nt) of F0 *Dnmt2* $^{+/+}$ and *Dnmt2*$^{-/-}$ males under ND and HFD. Value for each dot are generated by pooled sperm RNAs from 8 mice, as to reach enough RNA amount in each fraction to perform LC-MS/MS. Number of dots on the figure represents number of biologically independent experiments, which is also detailed in **Supplementary Table 1.** All data are plotted as mean±SEM (n = number of biologically independent experiments). All statistical analysis was performed by two-tailed, one-way Anova, uncorrected Fisher's LSD. All statistic source data and P values are provided in **Supplementary Table 1.**
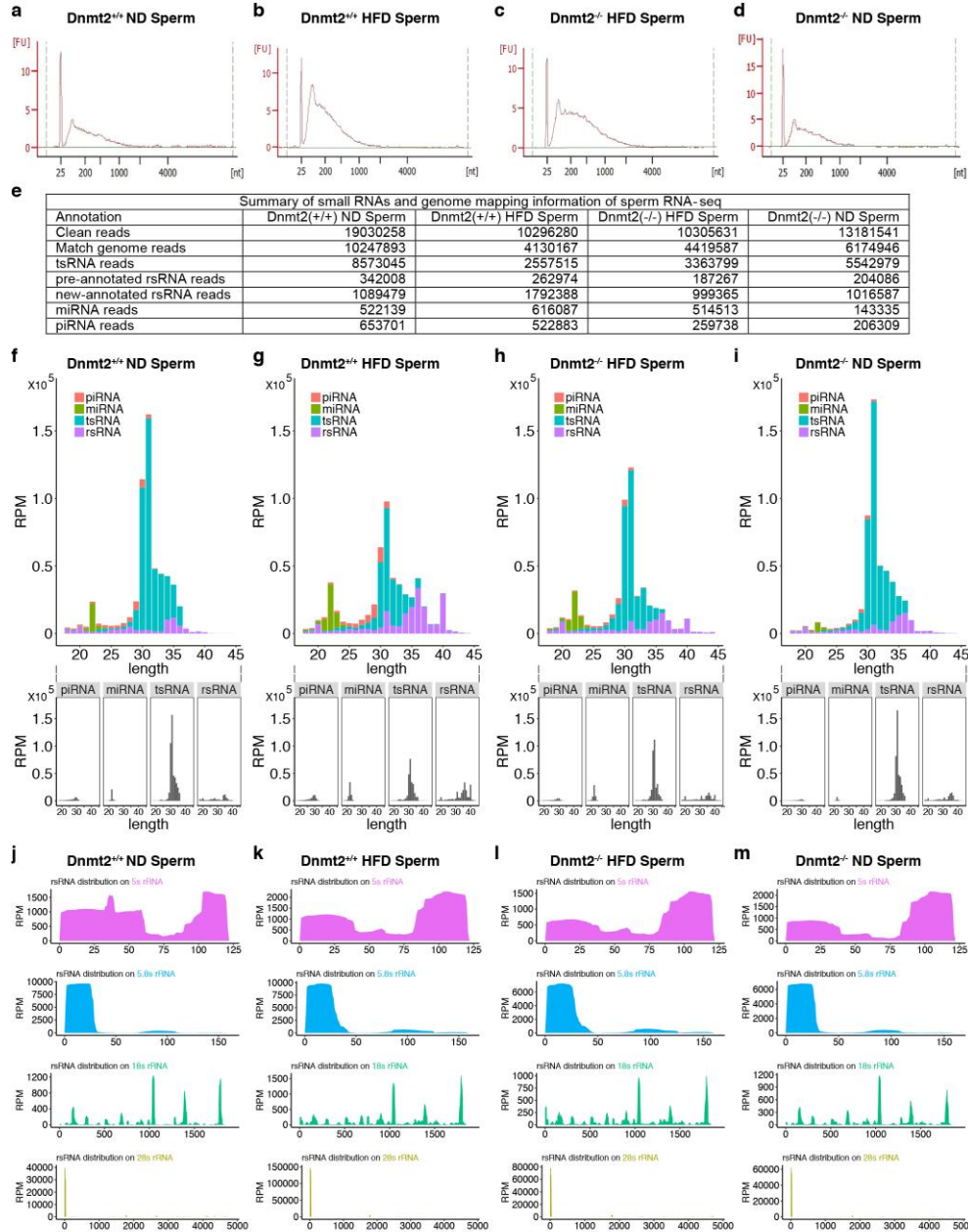
Supplementary Figure 3

Small RNA-seq analysis of sperm RNAs from F0 *Dnmt2*^{+/+} and *Dnmt2*^{-/-} males under ND and HFD.

The small RNA-seq quality control, statistics, and RNA profiling. (Data and images shown in this figure are representatives of two biological replicates, raw data for both replicates are archived in the Gene Expression Omnibus under accession number GSM2574268). **(a-d)** Electrophoretic size distribution of RNAs in **(a)** Dnmt2^{+/+} ND, **(b)** *Dnmt2*^{+/+} HFD, **(c)** *Dnmt2*^{-/-} HFD, **(d)** *Dnmt2*^{-/-} ND, analyzed by Agilent Bioanalyzer. **(e)** Summary of small RNA reads. Information for RNA reads annotation was analyzed by genome match information, miRNAs, piRNAs, tRNAs and rRNAs annotation according to mouse genome database (GRCm38/mm10), miRBase21[1], piRNA database[2, 3], GtRNAdb[4], NCBI Nucleotide database, Ensembl mouse ncRNA database (GRCm38/mm10) and Rfam 11.0 database [5]. **(f-i)** Length distribution and pattern changes of different sncRNAs (miRNAs, piRNAs, tsRNAs and rsRNAs) in **(f)** *Dnmt2*^{+/+} ND, **(g)** *Dnmt2*^{+/+} HFD, **(h)** *Dnmt2*^{-/-} HFD and **(i)** *Dnmt2*^{-/-} ND sperm. **(j-m)** loci mapping information of rsRNAs in different rRNAs (5sRNA, 5.8sRNA, 18sRNA and 28sRNA) for **(j)** *Dnmt2*^{+/+} ND, **(k)** *Dnmt2*^{+/+} HFD, **(l)** *Dnmt2*^{-/-} HFD and **(m)** *Dnmt2*^{-/-} ND sperm. RPM: reads per million.

Supplementary Figure 4

Dnmt2-depended m^{5}C modification regulate biological properties of tsRNA.

(a) Dnmt2-dependent C38 methylation in testis. Bisulfite sequencing maps for the three known tRNA targets of Dnmt2 (tRNA-Asp, tRNA-Gly and tRNA-Val) in mouse testis (*Dnmt2*$^{+/+}$ and *Dnmt2*$^{-/-}$). Each row represents one sequence read, each column a cytosine residue. Yellow boxes represent unmethylated cytosine residues; blue boxes indicate methylated cytosine residues (m^{5}C), sequencing gaps are shown in white. Numbers above the maps indicate the number of reads. Cytosine C38 is labeled in red, other cytosine sites are in black. **(b)** The sequence of chemically synthesized 3'tsRNA-Gly that harbors five m^{5}C according to the *Dnmt2*$^{+/+}$ condition (5 x m^{5}C), 3'tsRNA-Gly with four m^{5}C, lacking a Dnmt2-mediated m^{5}C at C38 position (4 x m^{5}C), and 3'tsRNA-Gly without any RNA modifications (no m^{5}C). **(c)** By transfecting the above three types of tsRNAs into 3T3 cell lines followed by transcriptome sequencing (n=2 biologically independent RNA samples). Each dot in the box plot represent the geneset score of one transcriptome data, the upper boundary of the box represents the maxima, the lower boundary represents the minima, and the centre represent the average. We observed that the same tsRNAs sequence with different number of m^{5}C modifications (no m^{5}C, five m^{5}C and four m^{5}C respectively) can induced different cellular transcriptome changes compared to the empty transfection: while all three types of tsRNAs similarly induced an overall elevated gene expression of Citrate Acid Circle pathway (which might be induced by and dependent on their specific sequence); the three types of tsRNAs with different m^{5}C modification induced distinct gene responses of Ribosome pathway (which might be sensitive to the RNA structural changes caused by m^{5}C), which may reflect recent studies reporting the function of tsRNAs in regulating Ribosome functions [6-9].

Fig. 4b Loading control

Fig. 4b 5' tsRNA-Gly

Fig. 4b 3'tsRNA-Gly

Fig. 4b 28s-rsRNA

Fig. 4d Denature PAGE gel

Fig. 4d Native PAGE - DMEM

Fig. 4d Native PAGE - RNase A/T1

Fig. 4d Native PAGE- DMEM and 20% FBS

Supplementary Fig. 1a

Supplementary Figure 5

Unprocessed gel blots.

Supplementary Table 1

Statistics Source Data

Statistic source data and P values for Fig. 1b-h, Fig. 2, Fig. 3a-c, Supplementary Fig. 1b,f,g,i-m, Supplementary Fig. 2, and a list of all type of RNA modifications examined.

Supplementary Table 2

Summary of outcome after different types of RNA injection into normal zygotes.